

1 **Preprint of** “The Largest Mountain Belt of the Last Billion Years:
2 The East African Orogen, its tectono-topographic evolution and
3 global significance.”

4 by

5 Collins, A.S.^{1*}, Blades, M.L.¹, Hasterok, D.¹, Cameron, F.¹,
6 Razakamanana, T.², Merdith, A. S.¹, Foden, J.D.¹, Clark, C.³

7

8 ¹Tectonics and Earth Systems (TES), Department of Earth Sciences, Adelaide
9 University, Adelaide, SA 5005, Australia. * = alan.collins@adelaide.edu.au

10 ²Département des Sciences de la Terre, Université de Toliara, Toliara, Madagascar

11 ³School of Earth and Planetary Sciences, Curtin University, Perth, Australia

12

13 This paper is a non-peer reviewed preprint submitted to EarthArXiv

14 This paper has been accepted for publication for publication
15 consideration In: Harley, S. (ed) *In the Footsteps of Hutton A celebration*
16 *of the tercentenary of the Birth of James Hutton*. Geological Society,
17 London, Special Publication.

18

19 The Largest Mountain Belt of the Last Billion Years: The East
20 African Orogen, its tectono-topographic evolution and global
21 significance.

22 Collins, A.S.¹, Blades, M.L.¹, Hasterok, D.¹, Cameron, F.¹, Razakamanana, T.², Merdith, A. S.¹,
23 Foden, J.D¹, Clark, C.³

24

25 ¹*Tectonics and Earth Systems (TES), Department of Earth Sciences, Adelaide University, Adelaide,*
26 *SA 5005, Australia.*

27 ²Département des Sciences de la Terre, Université de Toliara, Toliara, Madagascar

28 ⁵School of Earth and Planetary Sciences, Curtin University, Perth, Australia

29

30 **ABSTRACT**

31 Hutton's Principle of Uniformitarianism suggests that the present is the key to the past,
32 and in the present, Earth's topography is dominated by the Himalaya. The geological record
33 clearly preserves past mountain ranges, but few have purported to have the effect on Earth's
34 surface systems (such as the atmosphere, hydrosphere, biosphere and ocean chemistry) that the
35 Himalaya does today. The Neoproterozoic East African Orogen is an exception. Not only is it the
36 scale of the modern Himalaya, but it affected ocean chemistry in a similar manner to the
37 Himalaya. Here we posit that the East African Orogen is the only other Himalayan-scale mountain
38 range, and the only orogen that contends with the Himalaya as the largest mountain range of the
39 last billion years.

40 In this manuscript we review and reconstruct the orogen. We then use existing
41 metamorphic data triaged to exclude subduction-zone metamorphism, to estimate the
42 elevation-time evolution of the orogen. We demonstrate that the available metamorphic record
43 supports our assertion that the East African Orogen is amongst the largest orogens in the
44 geological record. We also integrate spatially-located metamorphic data with a full-plate tectonic

45 reconstruction of the evolving orogen to show how different plate interactions created the
46 evolving topography.

47

48 **INTRODUCTION**

49 Mountain belts transport material from the deep Earth to the reactive crucible of the planet's
50 surface, where it interacts with the atmosphere and hydrosphere and biosphere. This element-
51 transfer role of mountains controls such fundamental uniformitarian Earth processes as the
52 supply and extraction of CO₂ to and from the atmosphere, for example chemical weathering of
53 large mountain ranges can push the planet towards icehouse conditions (Godderis et al., 2017).
54 Weathering of mountain ranges also supplies nutrients that facilitate biological productivity and
55 help drive evolution (Cox et al., 2016b; Yang et al., 2020). A major step in understanding how our
56 planet evolved and developed as a system is to understand the history, location and evolution of
57 past mountain ranges (e.g. Merdith et al., Submitted).

58

59 We can track the fingerprints of past mountain ranges by variations in the products of extremely
60 long half-life radioactive decay systems into the oceans. The most useful of these is ⁸⁷Sr, which
61 forms by radioactive decay of ⁸⁷Rb that is relatively common in the lithosphere and has a suitably
62 long half-life of 4.92×10¹⁰ years. Strontium is soluble in water and has a residence time in the
63 oceans on the order of millions of years (Veizer et al., 1999; Vollstaedt et al., 2014), meaning that
64 it is well mixed in the oceans. It also readily precipitates with carbonates. These features mean
65 that strontium isotopes form an effective proxy for the erosion of old rocks—rocks that get
66 brought to the surface and eroded in mountain ranges. Therefore, the strontium isotope curve
67 for carbonates through the last billion years contains within it the globally homogenized orogenic
68 record through that time. For example, the growth of the Himalaya over the last 50 Ma is
69 reflected in a sharp rise in radiogenic strontium (Derry and France-Lanord, 1996). The only other
70 instance in the last billion years with a similar rise was between ca. 850–500 Ma, particularly
71 focused between ca. 660–500 Ma (Shields, 2007; Cox et al., 2016a; Chen et al., 2022). This period
72 coincides with the formation of the Gondwana-forming orogens (Collins and Pisarevsky, 2005;

73 Cawood and Buchan, 2007; Schmitt et al., 2018)(Fig. 1), of which the East African Orogen is the
74 largest in both spatial footprint and elevation (Fritz et al., 2013; Clark et al., 2015)(Figs. 1, 2).

75
76 Geographic reconstructions that divide the earth into land and sea have been a research focus
77 since the development of the continental drift hypothesis (Wegener, 1912). Palaeomagnetic-
78 based continental drift-like models that focus on continent distributions (Dalziel, 1997; Li et al.,
79 2008) have evolved into full-plate tectonic reconstructions that use the wealth of palaeotectonic
80 information held in global rock systems to attempt to reconstruct plate tectonics in deep time
81 (Domeier and Torsvik, 2014; Domeier, 2016; Merdith et al., 2017a; Merdith et al., 2021; Li et al.,
82 2023; Cao et al., 2024). Restoring the horizontal motion of Earth's lithosphere is not enough,
83 though, to accurately model the importance of the geosphere on Earth surface systems. We also
84 need to understand the geographic expression and distribution of Earth's surface topography
85 (and bathymetry). This has been attempted in the Phanerozoic by looking at preserved rocks and
86 attributing an elevation to that part of the world at the time of rock formation. For example, the
87 presence of preserved deep marine, shallow marine and terrestrial sedimentary rocks indicates
88 past flooded continents and coastal elevations. The presence of mountains is usually invoked
89 from the preservation of metamorphic rocks on the surface, exhumed by erosion of the orogenic
90 topography (e.g. Scotese, 2021). More quantitative approaches using the geochemistry of
91 igneous rocks that formed in specific tectonic settings (like volcanic arcs, or mountain belts) have
92 been developed that provide estimates of crustal thickness at the time of crystallisation, and
93 therefore information about past topography (Tang et al., 2021; Zhu et al., 2022; Zhou et al.,
94 2025). These approaches require magmatism, and many of the largest mountain ranges in the
95 world have limited magmatism during the times at which they have maximum elevation (e.g. the
96 Himalaya today). Here, we take a complementary approach to look at past-orogenic elevations,
97 by reviewing the pressure-time history preserved in metamorphic rocks and use these to
98 estimate past-orogenic elevation (Collins et al., 2022b).

99
100 In this manuscript, we first review the extent and nature of the preserved rocks within the East
101 African Orogen (Fig. 1), as one of the largest orogens known in the geological record, place them

102 within a modern full-plate tectonic framework, and qualitatively discuss the spatial and temporal
103 evolution of major topography. We aim that our method forms a focus for future investigations
104 into quantitative estimates of elevation to understand how orogenic evolution modulates Earth
105 system.

106

107 **THE CONCEPT OF THE EAST AFRICAN OROGEN**

108 The East African Orogen (EAO; Figs. 1, 2) was defined by Stern (1994). Here we restrict it to the
109 regions where rocks crop out or are found in the subsurface that were formed and/or deformed
110 in a mountain range that ran through the centre of Palaeozoic Gondwana (Fig. 1). The orogen
111 forms a broad band from northernmost Gondwana—Egypt and the Middle East, and now
112 dispersed terranes that reconstruct to this region—through eastern Africa and Madagascar (Figs.
113 1, 2). South of Madagascar, in reconstructed Gondwana, the orogen bifurcated into two branches
114 (Fig. 2). A western branch joins with the Zambezi Belt of Zambia and Zimbabwe and then to the
115 Lufilian Arc and the central Damara Belt (Goscombe et al., 2020)(Figs. 1, 2). An eastern branch
116 passes through southernmost India, Sri Lanka and into the Lützow-Holm Bay area of eastern
117 Antarctica (Plavsa et al., 2015) ('Lut' in Fig. 2). Here we will focus on the region north of this
118 bifurcation, where the EAO is clearly the result of ocean closure and subsequent continent-
119 continent collision between Neoproterozoic India and the Neoproterozoic African continents—
120 the southern Congo-Tanzania-Bangweulu continent and the Saharan metacraton (Figs. 1, 2). The
121 boundary between these two continents is the Central African Fold Belt (otherwise known as the
122 Oubanguides belt)(Figs. 1,2), which consists of a series of thrust sheets, known as the Yaoundé-
123 Yangana nappes (Toteu et al., 2022)("Y-Y" in Fig. 2) transported south over the Congo-Tanzania-
124 Bangweulu Block. The belt marks a site of ocean closure that separates a Neoproterozoic arc
125 terrane (Poli- Mayo Kebbi arc) from the Congo-Tanzania-Bangweulu continent and can be traced
126 west into the Sergipano belt of NE Brazil (Neves et al., 2006)(Fig. 1).

127

128 The EAO divided Gondwana into an eastern part, whose major components now form South
129 America and Africa, and a western part, whose now dispersed successors form Australia, East
130 Antarctica, India and much of East Asia (Fig. 1). In our discussion here we refer to directions in a

131 reconstructed Gondwana reference frame with Africa oriented as present day. The significance
132 of the EAO was increased when McWilliams (1981) supported early speculation that plate
133 tectonics operated in the Precambrian (Burke et al., 1976) and interpreted the palaeomagnetic
134 data of the times to reflect the existence of two large, separately travelling, continents that
135 collided to form Gondwana in the late Proterozoic. Stern (1994), delineated and named the EAO
136 and suggested that this was the site of collision between these east and west Neoproterozoic
137 Gondwana continents. This led to a hunt for the suture of the newly named Mozambique Ocean
138 that was hypothesized to have separated these continents (Shackleton, 1996).

139

140 In 1997, Ian Dalziel began the push to map the deep time geography of the planet by publishing
141 a major continental-drift style reconstruction for the Neoproterozoic (Dalziel, 1997) that
142 attempted to combine known geology with the palaeomagnetic record. This model coincided
143 with Joe Meert and Rob Van der Voo (1997) pointing out that the developing geochronological
144 record for the formation of Gondwana appeared to show three main periods of orogenesis. The
145 earliest orogeny, between 800–650 Ma, was correlated with the East African Orogeny and was
146 located mainly in East Africa. A second orogeny was interpreted as representing the
147 amalgamation of the South American part of Gondwana between 600–530 Ma. A third, eastern
148 Gondwanan orogeny, was suggested to have occurred at ca. 550 Ma. They named this the Kuunga
149 Orogeny and suggested that it involved the final amalgamation of Gondwana (Meert and Van der
150 Voo, 1997).

151

152 At about this time, several researchers realized that the vast region of the EAO preserved
153 evidence of considerable orogenic complexity, like that of Phanerozoic orogens. Kröner et al.
154 (2000) and Collins and Windley (2002) suggested that a major piece of pre-Neoproterozoic
155 continental crust lay within the East African Orogen. This palaeocontinent was subsequently
156 named 'Azania' (Collins and Pisarevsky, 2005) (Figs. 1, 2). It was proposed that Azania collided
157 with the Congo-Tanzania-Bangweulu continent at ca. 650 Ma and that this collision was the event
158 responsible for the East African Orogeny. Neoproterozoic India was hypothesized to have later
159 collided with the then combined Azania/Congo-Tanzania-Bangweulu continent at ca. 550 Ma

160 forming a Malagasy Orogeny (Collins and Pisarevsky, 2005). Meanwhile, Johnson and
161 Woldehaimanot (2003) published a key review of the northern EAO in the Arabian Nubian Shield
162 (Fig. 2). They demonstrated that this vast area, which incorporated all of Arabia and much of NE
163 Africa, consisted of a series of different-aged terranes that amalgamated at different times in a
164 similar, but better resolved, manner that Collins and coworkers were proposing in the southern
165 EAO. Johnson et al. (2011) and Fritz et al. (2013) published major reviews of the northern and
166 southern parts of the EAO.

167
168 The last 20 years has seen the identification of further pre-Neoproterozoic crust within the EAO
169 that has extended the number and complexity of continental terranes within the orogen (Be'eri-
170 Shlevin et al., 2009; Be'eri-Shlevin et al., 2012; Boger et al., 2014; Eyal et al., 2014; Boger et al.,
171 2015; Clark et al., 2020). Both margins of the EAO have been significantly revised and extended.
172 Here we suggest that the eastern margin be extended to include the basement of Oman,
173 Seychelles, Pakistan and NW India (Alessio et al., 2018; Blades et al., 2020; Collins et al., 2021b;
174 de Wall et al., 2022) (Figs. 1, 2). In these regions, juvenile Tonian (1000 to ca. 720 Ma, this and all
175 stratigraphic ages taken from Cohen et al., 2025) crust forms the basement, but in contrast to
176 the western EAO, orogenesis ended in the late Tonian or earliest Cryogenian (ca. 720–635 Ma).

177
178 The original definition of the western margin of the EAO as the boundary with a “Saharan
179 Metacraton” (Abdelsalam et al., 2002) is also far from clear and needs significant revision,
180 especially with the identification of Ediacaran (ca. 635–539 Ma) juvenile terranes in northern
181 Chad in the centre of the erstwhile “Saharan Metacraton” (Şengör et al., 2020; Shellnutt et al.,
182 2026). In Chad, a Neoproterozoic terrane has been identified and named the Poli-Mayo Kebbi-
183 Lake Fitri Terrane (PMKF)(Fig. 1). To date there are no pre-Neoproterozoic rocks known from this
184 region and it appears to be a juvenile Tonian terrane (Shellnutt et al., 2026). Southeast of the
185 PMKF lies the Adamawa-Yadé-Guéra-Ouaddaï (AYGO) Terrane (Fig. 1)(Shellnutt et al., 2026). This
186 contains gneisses with protoliths that date back to the Stenian (1000–1200 Ma)(Blades et al.,
187 2021), with detrital and inherited zircons that reach back to the Archaean (Djerossem et al., 2020;
188 Blades et al., 2021). These contrast with other parts of the Saharan basement, for example Gebel

189 Uweinat in SW Egypt, that preserve Archaean rocks that have largely missed later orogenesis
190 (Zhang et al., 2019)(Fig. 1). A boundary between pre-Neoproterozoic and Tonian crust marks the
191 edge of the EAO as shown in figures 1 and 2. Juvenile Neoproterozoic terranes then characterize
192 the western parts of the EAO (west of Afif-Abas and Azania, Fig. 2). The 800–650 Ma East African
193 Orogeny of Meert and Van der Voo (1997) affected these regions, but the later Malagasy Orogeny
194 (correlated with the Angudan Orogeny in Arabia, Collins and Pisarevsky, 2005) largely, did not
195 (with only local shear zones being active at this time).

196

197 The origin and tectono-geographic location of the EAO have been revised considerably. The
198 original suggestion, that the orogen preserved a Tonian continental rift sequence that
199 represented the break-up of Rodinia (Stern, 1994), is no longer tenable, as extensive Stenian crust
200 has been identified along the west margin of the EAO (de Wit and Linol, 2015; Blades et al., 2021)
201 and within the EAO in Madagascar, Sinai and East Antarctica (Eyal et al., 2014; Tucker et al., 2014;
202 Jacobs et al., 2015; Elburg et al., 2016; Archibald et al., 2018). In addition, the age of 800 Ma for
203 the beginning of the East African Orogeny (Meert and Van der Voo, 1997) is challenged by
204 extensive 850–750 Ma magmatism in central Madagascar (Handke et al., 1997; Archibald et al.,
205 2016; Archibald et al., 2017), pre-800 Ma magmatism in Ethiopia (Blades et al., 2015; Bowden et
206 al., 2020), Arabia (Whitehouse et al., 2016; Alessio et al., 2018), NW India and SE Pakistan (Pandit
207 et al., 2003; Shakoor et al., 2019), South India (Plavsa et al., 2015) and Sri Lanka (Kröner and
208 Jaeckel, 1994). A window into the basement in NE Oman demonstrates the presence of high-
209 grade metamorphism and deformation at ca. 820 Ma (Alessio et al., 2018) that links with pre-760
210 Ma tectonothermal activity recorded in the Pakistan and India basement west of the Western
211 Margin Fault of the Aravalli-Delhi Fold Belt India (Deb et al., 2001; de Wall et al., 2022), showing
212 that pre-800 Ma orogenesis is not limited to magmatism. We suggest that the orogen should now
213 be thought to represent over 500 million years of punctuated subduction-accretion. This new
214 paradigm means that the orogen does not represent a Wilson-like, internal ocean (Nance et al.,
215 1988), opening and closing in approximately the same position. Instead, it seems clear that the
216 orogen lay in a tectono-geographic position like that of the modern Pacific-rim, where subduction
217 of an external ocean over hundreds of millions of years resulted in a punctuated record of

218 accretion, extension, arc magmatism and collision (Merdith et al., 2017b; Şengör et al., 2020;
219 Collins et al., 2021b; Merdith et al., 2021). This process is similar to the Proterozoic to Mesozoic
220 history of the Central Asian Orogenic Belt (Kröner et al., 2014; Xiao et al., 2020) and the
221 Phanerozoic history of the Tasmanides of Australia and the broader Terra Australis Orogen
222 (Cawood, 2005; Glen and Meffre, 2009; Rosenbaum, 2018).

223
224 In the next section, we summarize the Stenian to Cambrian (ca. 1100–520 Ma) history of the now
225 dispersed parts of the EAO before we discuss the tectonic geography of their amalgamation and
226 evolution of the resulting mountain range(s).

227
228 **THE FAR NORTHERN EAST AFRICAN OROGEN**

229 ***Displaced terranes in Greece, Türkiye and Iran***

230
231 Tectonic windows into Neoproterozoic to early Palaeozoic crust occur as discontinuous
232 exposures throughout the central crystalline basement of Europe and from the Alps to Türkiye,
233 Syria and Iran in the Alpine–Mediterranean mountain belt (von Raumer et al., 2003). The
234 orogenesis preserved in these locations are variously attributed to the Cadomian or East African
235 orogen events (often just termed ‘Pan-African’). The precise original location of these now exotic
236 terranes are hard to define. However, the limited Mesozoic ocean crust development in the
237 western Mediterranean and (near?) continuity of the Apulia promontory with both northern
238 Gondwana and northern Europe means that the Aegean and eastern Mediterranean terranes are
239 restricted to originate close to the Egyptian margin of north Gondwana (Stampfli, 2005; Torsvik
240 and Cocks, 2013)(Fig. 2), close to where the East African Orogen met the circum-Gondwana
241 Ocean (which at this part of geological time and at this location is named the Tornquist Sea).

242
243 The terranes most pertinent here are the Greek Pelagonian Zone, the Turkish Tauride Terranes
244 (the Menderes Massif and the Bitlis Massif), as well as the dismembered terranes of the
245 Sanandaj–Sirjan Zone of Iran as these formed the far northern extensions of the EAO (Fig. 2). The
246 Pelagonian Zone of Greece contains the relatively small Florina Terrane, which preserves

247 orthogneisses dated as crystallizing between ca. 730–690 Ma (Anders et al., 2006). Crystallization
248 ages of this antiquity have not been recorded from the Menderes Massif that is found along
249 tectonic strike in west Türkiye. Here, an old kernel of Neoproterozoic clastic metasedimentary
250 rocks are intruded by 570–520 Ma granites (Gessner et al., 2004; Koralay et al., 2004) with rare
251 metabasites that preserve Cambrian eclogite metamorphic assemblages (Candan et al., 2016). A
252 similar Proterozoic clastic sequence is preserved in the Bitlis Massif of SE Türkiye, here also,
253 purported subduction-related magmatic rocks intrude the sequence at ca. 550–530 Ma
254 (Ustaomer et al., 2009). The Iranian Sanandaj-Sirjan Zone, contains a series of inliers of
255 Neoproterozoic–Cambrian metasedimentary rocks and granitoids decorating the Cenozoic
256 suture (Jamshidi-Badr et al., 2013; Fergusson et al., 2016; Honarmand et al., 2018). Further east
257 in Iran, the ‘Central and East Iranian Microcontinent’ (CEIM) consists of three blocks (the Lut,
258 Tabas and Yazd) separated by tectonic belts. In one of these belts, 575–525 Ma granitoids that
259 have been attributed to an Andean-like volcanic arc, suggest that this region shares a similar
260 Ediacaran–Cambrian tectonic setting to the other basement terranes in Türkiye and Iran
261 (Ramezani and Tucker, 2003; Rossetti et al., 2015). The continental volcanic-arc tectonic setting
262 of these has been questioned by Zoleikhaei et al. (2025), who argued that the detrital zircon and
263 apatite record in Ediacaran to Palaeozoic sandstones, is better explained by a rift setting at this
264 time with no arc-like edifice.

265
266 Both Ediacaran–Cambrian intrusions in the Sanandaj–Sirjan Zone and in the Menderes Massif
267 preserve inherited zircon that stretches back to ca. 3.6 Ga and hafnium isotopes on younger
268 grains that suggest ancient continent was a component of the source of these rocks (Nutman et
269 al., 2014). Whether this ancient source was crystalline basement beneath those regions, or
270 detritus then preserved in Proterozoic metasedimentary rocks is unclear.

271
272 **THE NORTHWESTERN EAST AFRICAN OROGEN: THE ARABIAN NUBIAN SHIELD (ANS)**
273 ***Egypt, Sudan, Saudi Arabia, Eritrea, central and north Ethiopia, Yemen, northern Somalia***

274

275 The ANS (Fig. 2) is dominated by low grade volcano-sedimentary sequences and associated
276 plutonic and ophiolitic remnants. These are reconstructed into a complex mix of terranes
277 representing accreted arcs that record subduction polarity reversals that are reviewed and
278 summarised in a number of papers (Johnson et al., 2011; Robinson et al., 2014; Kashghari et al.,
279 2025).

280

281 Pre-Stenian (> 1200 Ma) crust in the ANS forms two broad belts. One extends from the
282 Palaeoproterozoic Khida region of Saudi Arabia (which also underlies much of the Siham-Khida
283 Terrane—previously part of the Afif Terrane—to the north; Stoeser and Frost, 2006)(“SK” in Fig.
284 2) to the Abas Terrane of Yemen (Yeshanew et al., 2015; Whitehouse et al., 2023)(“Ab” in Fig. 2).
285 The Neoproterozoic Al-Bayda Terrane separates the Abas Terrane from the Palaeoproterozoic–
286 Archaean Al-Mafid Terrane of southern Yemen (“Ab” and “AMa” respectively in Fig. 2). The Al-
287 Mafid Terrane is traced south across to the Somaliland escarpment (Sassi et al., 1993), and
288 further south through eastern Ethiopia (Kröner and Sassi, 1996) to southern Somalia (Küster et
289 al., 1990), central Madagascar (Kröner et al., 2000) and into southern India (Collins and Windley,
290 2002; Collins et al., 2007; Plavsa et al., 2014)(Fig. 2). Collins and Pisarevsky (2005) named this pre-
291 Stenian microcontinent ‘Azania’ after the ancient Greek name for the east African Coast (Schoff,
292 1912).

293

294 The next oldest terrane in the ANS is the late Mesoproterozoic Sa’al Metamorphic Complex
295 (1.03–1.02 Ga) in Sinai, marking the initiation of magmatism in the northern-most Arabian
296 Nubian Shield (Be’eri-Shlevin et al., 2012; Eyal et al., 2014)(Fig. 2). The original location of this
297 Stenian terrane, is uncertain, due to it being surrounded by younger terranes, but coeval
298 subduction-magmatism occurred within the Saharan basement (Blades et al., 2021) and the Sinai
299 terrane may form a rifted part of this continent.

300

301 The Tonian to Cryogenian history of the ANS is marked by formation of oceanic volcanic arcs and
302 arcs built on Azanian (or Afif-Abas) crust that amalgamated to form a larger intra-Mozambique
303 Ocean terrane separate from both Neoproterozoic India and African Gondwanan continents. A

304 number of terranes in the ANS are correlated as equivalents, separated by the opening of the
305 Red Sea, from south to north, these are the Asir (a composite of the Bidah, An Nimas, Al Qarah-
306 Malahah and Tathlith terranes of Kashghari et al., 2025) and Tokar/Barka terranes, the Haya and
307 Jiddah terranes, the Hijaz and Gabgaba/Gebeit terranes, and the Eastern Desert and Midyan
308 terranes (Johnson et al., 2011)(Fig. 2). It is unclear whether the combined Asir-Tokar/Barka
309 terrane and Haya-Jiddah terranes were ever on separate plates as, in Saudi Arabia, no clear
310 suture is seen between them (Kashghari et al., 2025). In SE Sudan and Eritrea, the Tokar-Barka
311 Terrane (Fig. 2) has been subdivided into a number of smaller units (Drury and De Souza, 1998),
312 in a similar manner to its Saudi Arabian equivalent (Johnson et al., 2011). We suggest that these
313 terranes formed a complex middle Tonian continental amalgam.

314
315 The older, Tonian to earliest Cryogenian, amalgamation history of the ANS is marked by
316 approximately ENE-WSW oriented sutures (present orientation) between juvenile
317 Neoproterozoic ocean-arc terranes (Collins et al., 2021a; Collins et al., 2021b)(Fig. 2). The oldest
318 of these sutures is between the Jiddah-Haya and Gabgaba/Gebeit-Hijaz terranes (the Bi'r Umq-
319 Nakasib Suture)("bu" in Fig. 2), which is dated at ca. 780–750 Ma (Johnson et al., 2011). This
320 suture created the kernel of a late Tonian microcontinent. The Midyan-Eastern Desert terrane
321 collided with this kernel ca. 715 Ma along the Yanbu-Sol Hamed suture (Robinson et al., 2015a)
322 ("y" in Fig. 2). Both sutures evolved from SE-dipping subduction zones (Robinson et al., 2015a).

323
324 The older ENE-WSW sutures are bound by younger NNW-SSE oriented Cryogenian to Ediacaran
325 sutures and terranes that represent a fundamental kinematic change in Mozambique Ocean
326 subduction (Collins et al., 2021a; Collins et al., 2021b). The oldest of these is the 680–640 Ma
327 Nabitah Suture (Flowerdew et al., 2013)("ns" in Fig. 2), which forms the eastern margin of the
328 intra-Mozambique Ocean island-arc terrane microcontinent (discussed above), against Tonian-
329 Cryogenian continental arcs (Siham and Suwaj arcs of Kashghari et al., 2025)("SK" and "Sj" in Fig.
330 2) built on the Afif-Abas microcontinent. This now Cryogenian engorged Afif-Abas
331 microcontinent collided with the active margin of the Sahara basement along the Sudanese Keraf
332 Suture ("ks" in Fig. 2). This collision occurred in late Cryogenian to early Ediacaran times (ca. 650–

333 580 Ma)(Abdelsalam et al., 1998). Further to the east, in the most easterly exposed terrane—the
334 Saudi Ar Rayn Terrane—juvenile calc-alkaline magmatism stretches from ca. 690 Ma to 615 Ma
335 (Doebrich et al., 2007). Turbiditic sediment deposition in the Ad Dawadmi basin (“AD” in Fig. 2)
336 that separates the Ar Rayn Terrane (“AR” in Fig. 2) from the Afif-Abas microcontinent continued
337 until at least 620 Ma (Cox et al., 2012), but was locally intruded by ca. 630 Ma adakitic magmas
338 (Cox et al., 2019). This sequence was metamorphosed to greenschist-facies grades at ca. 620 Ma
339 (Cox et al., 2012). Further east still, broad N–S magnetic highs, beneath the Arabian Phanerozoic
340 sedimentary sequence (Johnson and Stewart, 1995), suggest younger arc terranes now buried
341 beneath the Rub al-Khali Basin (Fig. 2). Geochronological data from basement-intercepting
342 boreholes throughout Saudi Arabia exclusively yield Neoproterozoic ages from these buried
343 terranes (Collins et al., 2024). Deformation that we interpret as related to the collision and
344 amalgamation of these buried terranes is prominent in the subsurface of western Oman where
345 it is known as the Western Deformation Front (“WDF” in Fig. 2) and delineates the Angudan
346 Orogeny (Loosveld et al., 1996; Al-Barwani and McClay, 2008; Gómez-Pérez and Morton, 2025).
347 We correlate this latest Ediacaran–Cambrian Angudan Orogeny with the Malagasy Orogeny of
348 Collins and Pisarevsky (2005). This event is interpreted as the final suture of the Mozambique
349 Ocean (Gómez-Pérez et al., 2024; Gómez-Pérez and Morton, 2025). A zone of lithospheric mantle
350 shear wave anisotropy in far southwestern Oman may locate this suture in the upper mantle (Al-
351 Lazki et al., 2012), this broadly correlates with highly strained Ediacaran volcano-clastics found in
352 the subsurface and at outcrop (Gómez-Pérez and Morton, 2025). Al Rawahi et al. (2026)
353 demonstrated from provenance changes in the late Ediacaran Fara Formation of Oman that
354 closure of this suture occurred by ca. 551 Ma. In contrast, the transition to post-tectonic
355 magmatism within the eastern terranes of the Arabian Nubian Shield begins much earlier, from
356 ca. 605 Ma, with post-tectonic magmatism (Doebrich et al., 2007; Cox et al., 2012; Robinson et
357 al., 2014; Robinson et al., 2015b; a; Cox et al., 2019) and pull-apart basins developed along the
358 large strike-slip faults (known as the Najd Faults) that cut the region (Moore, 1979; Meyer et al.,
359 2014; Nettle et al., 2014; Shen et al., 2022; Hamimi et al., 2023).

360

361 The basement of Yemen is marked by considerable pre-Neoproterozoic crust found in the Al-
362 Mahfid and Abas terranes (Windley et al., 1996; Whitehouse et al., 1998). The Abas terrane is
363 linked with the Siham-Khida Terrane of Saudi Arabia (Whitehouse et al., 1998; Yeshanew et al.,
364 2015) to form the Afif-Abas continent of Collins and Pisarevsky (2005)(Fig. 2). Whereas the Al-
365 Mahfid Terrane has been linked with pre-Stenian crust found through Somaliland, eastern
366 Ethiopia, southern Somalia, central Madagascar and the Madurai Block of southern India that
367 formed the continent Azania (Whitehouse et al., 2001; Collins and Pisarevsky, 2005). The Abas
368 Terrane lies east of an interpreted late Tonian to Cryogenian arc, called the Amlah Terrane
369 (Whitehouse et al., 2025)(“Aml” in Fig. 2) and an oceanic suture between this and the Saudi
370 Arabia Tathlith Terrane (Kashghari et al., 2025) is inferred by the change in younging direction of
371 preserved volcanic arc intrusions (Flowerdew et al., 2013; Whitehouse et al., 2025). The Abas
372 Terrane is largely composed of ca. 790–725 Ma granitic gneisses with variable $\epsilon(\text{Nd})_t$ values as
373 evolved as -11, suggesting significant ancient crust in the source magmas (Whitehouse et al.,
374 1998; Yeshanew et al., 2015). Some rocks may date back to the early Tonian and a single
375 Neoproterozoic core has been analysed hinting at the age of older basement (Whitehouse et al.,
376 1998). The juvenile Al Bayda Terrane (“ABa” in Fig. 2) separates the Abas Terrane from the Al
377 Mahfid Terrane. The latter contains significant Neoproterozoic crust and was interpreted by Collins
378 and Windley (2002) to form the northern part of a Neoproterozoic continent that lies within the
379 EAO (Azania of Collins and Pisarevsky, 2005). The Al Mukalla Terrane (“Amk” in Fig. 2) lies east of
380 the Al Mahfid in Yemen and was correlated by Whitehouse et al. (2001) with the Maydh (or Mait)
381 Terrane of northern Somalia (Somaliland)(“M” in Fig. 2), which contains meta-tholeiitic basalts
382 with pillow-lavas textures and mid-ocean ridge like chemistries (Dal Piaz et al., 1993).

383
384 Pre-Neoproterozoic rocks are found along the southern escarpment margin of the Gulf of Aden
385 in northern Somalia (Somaliland) and eastern Ethiopia form a > 600 km long inlier between the
386 latitudes of 41–47° E, from Hirna in east Ethiopia to the town of Maydh in northern Somalia.
387 These were included within Azania by Collins and Pisarevsky (2005). In Somaliland, the oldest
388 components of this inlier are the Qabri Bahar and Mora complexes (Sassi et al., 1993)(“QM” in
389 Fig. 2), which consists of paragneisses and orthogneisses with local migmatites and granulite-

390 facies relics (Sassi and Visonà, 1993). The east Ethiopian continuation of this belt makes-up the
391 unimaginatively named 'Lower Unit' and Bora Group of the Harar-Hirna area (Kazmin, 1975;
392 Berhe, 1981)("HH" in Fig. 2) that contain ca. 2000 Ma tonalitic gneiss xenoliths in Tonian
393 granitoids (Teklay et al., 1998; Yeshanew et al., 2017). In addition, Archaean and earliest
394 Palaeoproterozoic zircon grains have been reported from granitoids interleaved with
395 metasedimentary gneisses (Teklay et al., 1998). All analysed rocks in eastern Ethiopia have
396 evolved neodymium isotope values, suggesting that either there are older rocks at depth, or that
397 the metasedimentary protolith source was derived from more ancient crust, or both (Teklay et
398 al., 1998; Yeshanew et al., 2017).

399
400 In Eritrea, the Tokar/Barka Terrane (Johnson and Woldehaimanot, 2003) consists of juvenile 850–
401 650 Ma old supracrustal and intrusive rocks that range from low greenschist facies to granulite
402 facies (Andersson et al., 2006). Peak metamorphism of these rocks is dated at ca. 590 Ma
403 (Andersson et al., 2006). Rocks of the Tokar/Barka Terrane in Eritrea pass south into the Tsaliet
404 Group of Tigray in northern Ethiopia where they conformably pass up into Tonian strata of the
405 Tambien Group that are well dated to between ca. 820 Ma and < 719 Ma (Swanson-Hysell et al.,
406 2015; Park et al., 2019). This region has missed the high-grade Ediacaran metamorphism seen
407 both to the east and west.

408
409 To the southwest, the Western Ethiopian Shield (WES) is one of the larger regions of ANS outcrop
410 (Fig. 2). It marks the transition from the relatively low-grade ANS to the higher metamorphic
411 grades of the Mozambique Belt (Abdelsalam and Stern, 1996). The WES preserves no evidence
412 of pre-Neoproterozoic crust, with the oldest rocks in the area dated at ca. 855 Ma (Blades et al.,
413 2015) with geochemical evidence suggesting that they formed above an intra-oceanic subduction
414 zones (Blades et al., 2019). Magmatism (re-melting of juvenile crust) and deformation is seen at
415 810–770 Ma and at 660–635 Ma in the Western Ethiopian Shield, with post tectonic magmatism
416 at ca. 584 Ma (Blades et al., 2015; Blades et al., 2019; Bowden et al., 2020). All the rocks in the
417 Western Ethiopian Shield have juvenile $\epsilon\text{Hf}(t)$ values of +4.5 to +10, suggesting that the influence
418 of continental crust was minimal.

419
420
421
422
423
424
425
426
427
428
429
430
431
432
433
434
435
436
437
438
439
440
441
442
443
444
445
446
447

THE WESTERN MARGIN OF THE EAST AFRICAN OROGEN

Sudan, Chad, Central African Republic, South Sudan, Uganda

The western margin of the East African Orogen can be reasonably well located in northern Sudan where > 900 Ma schists and gneisses are overthrust by 800–900 Ma gneisses and low-grade metavolcanic rocks of the Rahaba–Absol Terrane (Harms et al., 1994; Schandelmeier et al., 1994; Johnson and Woldehaimanot, 2003) (“RA” in Fig. 2). Thrusting was over here before 700 Ma (Abdelsalam et al., 1995). As you get further south, though, the western margin becomes hard to locate as much of the south-east of the region often denoted as the Sahara Metacraton (Abdelsalam et al., 2002) has a basement made up of late Mesoproterozoic rocks that formed in volcanic arc terranes (Shellnutt et al., 2017; Blades et al., 2020; Djerossem et al., 2020; Plunder et al., 2026). This suggests that this part of the basement to Chad and Sudan forms an earlier accretionary orogen that simply gets younger eastward into the EAO—part of a large and long-lived accretionary system, possibly stretching to the eastern edge of the West African Craton (Şengör et al., 2020; Lom et al., 2024; Shellnutt et al., 2026).

The Nuba Mountains lie at a critical point to the west of the traditional western boundary of the EAO, yet north of the Ediacaran tectonism that marks the Central African Fold Belt (Fig. 2). The eastern part of the exposed basement rocks consist of low-grade volcano-sedimentary rocks that are separated from a higher-grade gneiss terrane in the central Nuba Mountains by the Kabus ophiolitic mélange (Abdelsalam and Dawoud, 1991). This boundary has long been used to mark the western boundary of the ANS and therefore the East African Orogen (Abdelsalam and Dawoud, 1991; Johnson and Woldehaimanot, 2003). Mohammed (2017), however, showed that these gneisses are Neoproterozoic and to the west of them lies a ca. 780 Ma ophiolitic succession that he named the Arid Unit. This suggests that juvenile Neoproterozoic crust continues west of the Nuba Mountains and that these mountains lie close to the triple junction where the EAO meets the Central African Fold Belt (Fig. 2).

448 **THE NORTHEASTERN EAST AFRICAN OROGEN**

449 ***NW India, Pakistan, Oman, UAE, Afghanistan, SE China, Seychelles, N Madagascar***

450

451 There are three main windows into the Omani basement exposed east of the ‘Western
452 Deformation Front’. These all lie east of the possible lithospheric suture marked by shear wave
453 splitting in far southwestern Oman mantle (Al-Lazki et al., 2012). The tectonic windows are Al
454 Jobah (northern Huqf area), Jebel Ja’Alan (NE Oman) and Mirbat region of Dhofar in the south-
455 east (“Hu”, “JJ” and “Mir” in Fig. 2). These have been interpreted to represent arc accretion
456 during the Tonian (890–720 Ma) (Stern and Johnson, 2010; Rantakokko et al., 2014; Whitehouse
457 et al., 2016; Alessio et al., 2018), with magmatism and deformation/metamorphism broadly
458 younging from the NE to the SW, towards the putative final Mozambique Ocean suture (Blades
459 et al., 2020). In addition, clasts brought up from > 8km depth in salt diapirs in Oman and the United
460 Arab Emirates preserve volcanic rocks with ages between 560–545 Ma that contain inherited
461 zircons back to the Neoproterozoic (Thomas et al., 2015). Detrital zircons in sedimentary enclaves
462 show a similar age range (Thomas et al., 2015; Arboit et al., 2024) as do in-situ metasedimentary
463 basement rocks of the Jebel Ja’Alan region (Whitehouse et al., 2016; Blades et al., 2020). These
464 suggest a depositional connection to crust of considerable antiquity. A number of workers have
465 suggested that Afghanistan may be possible source for these (Thomas et al., 2015; Alessio et al.,
466 2018; Blades et al., 2020), as this Archaean/Palaeoproterozoic terrane likely lay with the NW
467 Neoproterozoic Indian accretionary system and was interpreted in Merdith et al. (2021) as
468 correlating with the SW of the Yangtse craton of China as a microcontinent accreted to the
469 Neoproterozoic Indian margin in the Tonian.

470

471 In Gondwana, Oman lay adjacent to NW India in Gondwana (Figs. 1, 2), and by Ediacaran times,
472 at least, a similar sedimentary package was deposited across Rajasthan, Pakistan and through
473 Oman that contains excellent petroleum source rocks and evaporites (Cozzi et al., 2012). These
474 were being deposited in a stable, passive margin environment (Allen, 2007) at the same time that
475 rocks in the eastern Saudi Arabian Shield were forming in an active subduction margin (Cox et al.,
476 2012). The pre-Ediacaran basement rocks in Rajasthan and Pakistan, also, share similarities with

477 those of Oman. Granitoids have been dated from Rajasthan (“Raj” in Fig. 2) and from Nagar
478 Parkar in eastern Sind (Pakistan, “NP” in Fig. 2) at ca. 1.1 Ga (Raza et al., 2012; Meert et al., 2013).
479 But no evidence of pre-existing crust occurs west of the Western Margin Fault of the Aravalli-
480 Delhi Orogen (“wmf” in Fig. 2). Tonian granitoids and rhyolites occur in inliers through northwest
481 India and Pakistan, where they cluster into crystallization ages of ca. 990–970 Ma (Pandit et al.,
482 2003), ca. 860–820 Ma (Davies and Crawford, 1971; Deb et al., 2001; Van Lente et al., 2009; Just
483 et al., 2011) and ca. 775–760 Ma (Gregory et al., 2009; Van Lente et al., 2009; Ashwal et al., 2013;
484 Meert et al., 2013). The latter magmatic and extrusive phase forms one of the largest felsic
485 igneous provinces on the planet, which is also traced to the Seychelles (Torsvik et al., 2001;
486 Tucker et al., 2001)(“Sey” in Fig. 2), and may correlate with the northern Bemarivo Belt of
487 Madagascar where the magmatism dates from ca. 750–705 Ma (Collins, 2006; Thomas et al.,
488 2009; Armistead et al., 2019)(“Bem” in Fig. 2).

489
490 Armistead et al. (2019), showed that ca. 750–705 Ma rocks from the northern Bemarivo Belt of
491 far north Madagascar preserve similar juvenile $\epsilon\text{Hf}(t)$ signatures to rocks in south China,
492 Rajasthan, Oman and the Seychelles, that had previously been suggested to have formed a
493 volcanic arc system on the margin of Neoproterozoic India (Wang et al., 2017; Cawood et al.,
494 2018). The period of magmatism in this proposed arc was long-lived, beginning at around ca. 850
495 Ma and ending at around ca. 700 Ma. When reconstructed in this fashion (Armistead et al., 2019),
496 there is a general southward to southeastward younging trend (reconstructed orientation), with
497 the oldest record coming from China, and progressing to younger rocks through Oman, Malani,
498 Seychelles and the northern Bemarivo Belt.

499
500 Tonian palaeomagnetic data from Oman (Swanson-Hysell et al., 2025; Antonio et al., 2026)
501 support the correlation of Oman with Neoproterozoic India at the time (Alessio et al., 2018).
502 Sedimentological data from the Cryogenian and Ediacaran deposits suggest that this link lasts
503 through until Ediacaran formation of Gondwana (Cozzi et al., 2012; Gómez-Pérez et al., 2024;
504 Gómez-Pérez and Morton, 2025). Only colliding with the rest of Arabia in the late Ediacaran

505 (Collins and Pisarevsky, 2005; Blades et al., 2020; Merdith et al., 2021; Cao et al., 2024; Gómez-
506 Pérez and Morton, 2025; Al Rawahi et al., 2026).

507

508 **THE CENTRAL EAST AFRICAN OROGEN**

509 ***Southern Ethiopia, Uganda, Kenya, NE Tanzania, southern Somalia***

510

511 The grade of metamorphism of rocks exposed on the surface increases through Ethiopia from
512 the broadly greenschist-facies rocks of the ANS in the north to upper amphibolite and granulite-
513 grade rocks that dominate the Mozambique Belt south of central Ethiopia. We interpret this
514 transition to reflect greater Cryogenian to Cambrian orogenesis in the south with higher and
515 more extensive orogenic topography of the overlying mountains (see discussion below for more
516 on palaeoelevation).

517

518 South of the Western Ethiopian Shield (WES, Fig. 2), the Karamoja Belt of NE Uganda (“Kmja” in
519 Fig. 2) is dominated by the Karasuk Supergroup (Vail, 1985; Westerhof et al., 2014), which are
520 metaigneous rocks that crystallized between ca. 740 Ma and ca. 680 Ma (Mänttäre et al., 2011;
521 Westerhof et al., 2014) and are intruded by post-tectonic granitoids with U–Pb crystallization
522 ages of ca. 660 Ma (Mänttäre et al., 2011). Similar timing of magmatism is seen within the WES
523 (Blades et al., 2015), however, there is a notable difference between the Southern Ethiopian
524 Shield (“SES” in Fig. 2) and the Karamoja Belt. In the Southern Ethiopian Shield, a ca. 660 Ma
525 event that is coeval with the late magmatism in the eastern WES, is termed the ‘Moyale Event’
526 (Teklay et al., 1998) this is associated with multiply deformed dismembered ophiolites (Abebe et
527 al., 2025). Further east still, Yeshanew et al. (2017) identified Ediacaran granitic magmatism (600
528 – 560 Ma) in the Harar region of eastern Ethiopia (“HH” in Fig. 2). The Ediacaran ages extend
529 known magmatic events in the region to much younger ages than previously reported, and
530 considerably younger than any orogenesis in the Western Ethiopian Shield. Two of the granitoid
531 samples dated at ca. 600 and ca. 585 Ma are not deformed, whereas the younger gneisses at ca.
532 568 and ca. 560 Ma are strongly deformed. These were interpreted to represent a low-strain
533 domain during orogenesis (Yeshanew et al., 2017) and suturing between two lithospheric blocks

534 (WES and Eastern Ethiopia—Azania?). These mid-late Ediacaran ages are much younger than any
535 evidence for tectonism found in the WES, and any suggested ocean closure from the ANS west
536 of the Saudi Arabian Afif Terrane (Johnson et al., 2011), so rather than representing suturing
537 between the WES and eastern Ethiopia, we suggest that the post-ca. 560 Ma deformation may
538 reflect late intra-continental deformation, as seen elsewhere in the ANS (e.g., Kusky and Matsah,
539 2003).

540

541 To the south, in Kenya, southern Somalia and Tanzania, the East African Orogen is dominated by
542 high-grade gneisses of the Mozambique Belt (see Fritz et al., 2013 for a review)(“Moz Belt” in Fig.
543 2). In the region of the town of Lodwar in NW Kenya (“Ld” in Fig. 2), amphibolite-grade
544 orthogneisses yield protolith ages of ca. 800 Ma that were metamorphosed at ca. 630 Ma (Blades
545 et al., 2026). These are separated from the NE edge of the Congo-Tanzania-Bangweulu Block by
546 the Cryogenian to early Ediacaran West Pokat ophiolite (Vearncombe, 1983; Ries et al.,
547 1992)(“Pok” in Fig. 2) and are themselves bound to the east by metasedimentary gneisses that
548 record peak metamorphic conditions of 8.4–10.6 kbar and temperatures of 750–830°C at ca. 625
549 Ma (McIntyre, 2023). The Lodwar orthogneisses likely correlate north with the Didesa Terrane
550 (West Ethiopian Shield; Blades et al., 2015). This region passes south into the Western Granulites
551 of SW Kenya and Tanzania (“WG” in Fig. 2) that involve highly metamorphosed pre-
552 Neoproterozoic crust that was metamorphosed to granulite facies at ca. 630–615 Ma (Möller et
553 al., 2000; Sommer et al., 2003; Cutten et al., 2006; Apen et al., 2020) and locally extruded
554 westward over the Congo-Tanzania-Bangweulu Block (Eguíluz et al., 2024).

555

556 The eastern part of the Mozambique Belt (Burr Massif, Somalia, Fig. 2) consists of a tract of largely
557 pre-Neoproterozoic continental crust, strongly deformed, partially melted and metamorphosed
558 in the Ediacaran/Cambrian (ca. 600 and ca. 530 Ma, Küster et al., 1990; Lenoir et al., 1994).
559 Extensive tectonothermally reworked pre-Neoproterozoic crust lies further west in the
560 Neoproterozoic Tanzanian craton (Muhongo et al., 2001; Johnson et al., 2003; Reddy et al., 2003;
561 Tenczer et al., 2013). Near peak, granulite-grade metamorphism along the western part of this
562 belt (ca. 640 Ma), has been dated by metamorphic zircons (Coolen et al., 1982; Muhongo, 1994;

563 Appel et al., 1998; Muhongo et al., 2001). Hauzenberger et al. (2007) identified that the age of
564 metamorphism further east, in the Galana River area (“GR” in Fig. 2), is considerably younger
565 (580–530 Ma) overlapping the age of the ‘Malagasy Orogeny’ of Collins and Pisarevsky (2005).

566

567 **THE SOUTHERN EAST AFRICAN OROGEN: THE MOZAMBIQUE BELT AND THE EAST AFRICAN** 568 **OROGEN BIFURCATION**

569 *Tanzania, northern Mozambique, Madagascar*

570

571 In Gondwana, Madagascar lay directly off the east coast of Tanzania and SE Kenya (Reeves et al.,
572 2004)(Figs. 1, 2). Terranes in this area have been tentatively extended into western Madagascar
573 (Fritz et al., 2013). For example, in the South Kenyan Galana River region, the Sobo Unit has been
574 correlated with the pre-Neoproterozoic terranes of western Madagascar, while the Galana and
575 Sagala Units are linked with the Vohibory Terrane of far SW Madagascar (Fritz and Hauzenberger,
576 2021)(“V” in Fig. 2). The Rantosara shear zone of southern Madagascar also has been correlated
577 with deformation along the Galana-Mutito Shear Zone (Hauzenberger et al., 2007). Unlike the
578 Ranotsara shear zone (“rsz” in Fig. 2), though, the Galana-Mutito Shear Zone separates distinct
579 terranes with different protolith origins and histories (Schreurs et al., 2010; Fritz et al., 2013; Fritz
580 and Hauzenberger, 2021). To the east of the Galana-Mutito Shear Zone lies the microcontinent
581 Azania (Fig. 2), whereas to the west are a series of Neoproterozoic terranes known as the Kasigau
582 and Kurase Units in Kenya (Frisch and Pohl, 1986), the Eastern Granulites in Tanzania (Maboko,
583 2000)(“EG” in Fig. 2) and the Cabo Delgado Nappe Complex in northern Mozambique (Viola et
584 al., 2008)(“CD” in Fig. 2). These originated as Neoproterozoic volcanic arcs that consumed the
585 western branch of the Mozambique Ocean (Kröner et al., 2003; Cutten et al., 2006; Mole et al.,
586 2018; Fritz and Hauzenberger, 2021).

587

588 Subduction of a strand of the Mozambique Ocean that separated the
589 Congo/Tanzania/Bangweulu continent from Azania began as early as 1080 Ma with the formation
590 of an intra-oceanic volcanic arc that is preserved today as the ca. 1080–980 Ma Dabolava Arc of
591 western Madagascar (Tucker et al., 2014; Archibald et al., 2018)(“Db” in Fig. 2). This arc system

592 can be traced south in reconstructed Gondwana into the ‘Tonian Oceanic Arc Superterrane’
593 (TOAST) region of East Antarctica (Jacobs et al., 2015; Merdith et al., 2017b; Merdith et al.,
594 2021)(Fig. 2). Later formed, early Tonian, supra-subduction arc systems included magmatism on
595 the surrounding pieces of continental crust as well as within the ocean itself. These include the
596 Galana and Sagala units with emplacement ages between 970 Ma and 850 Ma and the ca. 930–
597 900 Ma Vohibory arc terrane of SW Madagascar (Jöns et al., 2005; Jöns and Schenk, 2008; Collins
598 et al., 2012)(Fig. 2). Protoliths to granulites in the Pare–Usambara and Uluguru Mountains (“Ulu”
599 in Fig. 2) of Eastern Tanzania preserve subduction-related magmatism dated to ca. 700–800 Ma,
600 which is broadly coeval with the extensive 850–750 Ma Itsindro-Imerona arc that intruded
601 throughout central Madagascar (Handke et al., 1997; Archibald et al., 2016; Archibald et al.,
602 2017). Finally, the youngest known subduction-arc terrane in this area forms the ca. 700–650 Ma
603 Ntaka terrane of southern Tanzania (Mole et al., 2018)(“Nt” in Fig. 2).

604
605 In Madagascar, accreted Late Mesoproterozoic to Tonian arc systems make up much of the
606 western part of the exposed basement of the island (Collins, 2006; Tucker et al., 2014; Archibald
607 et al., 2018; Boger et al., 2019; Collins et al., 2022a). The central part of Madagascar (the
608 Antananarivo Domain, “Tana” in Fig. 2) forms a pre-Neoproterozoic continent made up of
609 Archaean orthogneisses (Tucker et al., 1999; Tucker et al., 2011; Armistead et al., 2018; Archibald
610 et al., 2023), overlain and interleaved with Palaeoproterozoic and Mesoproterozoic sequences of
611 meta-sedimentary rocks (Cox et al., 1998; Cox et al., 2004; Archibald et al., 2015; Armistead et
612 al., 2021; Costa et al., 2021). To the east of this pre-Neoproterozoic unit lies a series of
613 Neoproterozoic metasedimentary rocks that include pods of ultramafic rocks (the Anaboriana-
614 Manampotsy belt). These rocks separate central Madagascar from the Antongil and Masora
615 domains (“At” and “Ms” in Fig. 2, respectively); the former, at least, is a displaced part of the
616 Western Dharwar Craton (Tucker et al., 1999; Boger et al., 2014; Tucker et al., 2014; Armistead
617 et al., 2018). Collins et al. (2003) suggested that the Anaboriana-Manampotsy belt forms a cryptic
618 suture (the Betsimisaraka Suture, “bet” in Fig. 2) between a Neoproterozoic continent (named
619 ‘Azania’ by Collins and Pisarevsky, 2005) and Neoproterozoic India (Collins and Windley, 2002).
620 This interpretation was countered by Tucker et al. (2011; 2014) who argued that central

621 Madagascar was a continuation of the Dharwar Craton and that the Anaboriana-Manampotsy
622 belt originated as an intra-continental basin. The Anaboriana-Manampotsy belt passes north to
623 the Bemarivo Domain of far north Madagascar (Collins and Windley, 2002)(“Bem” in Fig. 2). Here,
624 Armistead et al. (2019) demonstrated that the northern part of this region formed a juvenile ca.
625 750–700 Ma terrane that they named the Bobakindro Terrane. These authors argued that it
626 formed a continuation of the volcanic arc terranes that accreted to Neoproterozoic India during
627 the Tonian and Cryogenian (Blades et al., 2020; Collins et al., 2021b) and correlated south with
628 the Betsimisaraka Suture to separate Neoproterozoic India from Azania and African-derived
629 terranes.

630
631 The foreland to the Lurio Belt of northern Mozambique consists of the Stenian Nampula Complex
632 (“Na” in Fig. 2), which is relatively weakly deformed and metamorphosed in the Neoproterozoic
633 (Kroner et al., 1997; Sacchi et al., 2000; Bingen et al., 2009). The Lurio foreland disrupts the
634 orogenic trend of the EAO and splits it into southwestern and southeastern branches with a triple
635 junction that lay directly south of Madagascar and Southern India (Schmitt et al., 2018; Clark et
636 al., 2020)(Figs. 1, 2). The southwestern branch passes through Malawi and as it tracks further
637 west, it is progressively known as the Zambezi Belt, the Lufilian Arc (Fig. 2) and eventually the
638 Central Damara Orogen in Namibia (“Da” in Fig. 1). The southeastern branch forms a broad
639 orocline, curving through Sri Lanka where it encompasses the Wannii and Highland Complexes
640 (“W” and “HC” in Fig. 2, respectively). The orocline wraps around the Stenian Vijayan Complex
641 (correlated with the Nampula Complex by Collins and Pisarevsky, 2005)(“V” in Fig. 2) and passes
642 into East Antarctica in the region of Lutzöw Holm Bay (“Lut” in Fig. 2).

643

644 **THE SOUTHWEST BRANCH OF THE EAST AFRICAN OROGEN**

645 ***Northern Mozambique, Malawi, Zambia***

646 Northern Mozambique and southeastern Zambia experienced extension and deposition in the
647 early Neoproterozoic. Metasedimentary units in the Marrupa and Unango complexes of
648 Mozambique (Bingen et al., 2009)(“M-U” in Fig. 2) and the Nyimba-Sinda Terrane of Zambia
649 (Alessio et al., 2019a)(“N-S” in Fig. 2) likely reflect basin development contemporaneous with late

650 Tonian/early Cryogenian rift-related magmatism in NE Mozambique (Bjerkgard et al., 2009),
651 Malawi (Ashwal et al., 2007) and east Zambia (Johnson et al., 2006). This rifting is interpreted as
652 associated with the breakup of central Rodinia and connected with the initial opening of the
653 Pacific Ocean basin (Merdith et al., 2017a). Subsequent collision between the Kalahari continent
654 and the Congo-Tanzania-Bangweulu Block formed some of the younger orogenesis that made-
655 up Gondwana (Schmitt et al., 2018; Gomes et al., 2025). Peak metamorphism within the central
656 Damara Orogen (“Da” in Fig. 1) culminated at 530–525 Ma (Goscombe et al., 2017), which
657 matches similar Cambrian peak metamorphism in the Zambezi Belt (John et al., 2004). Post-peak
658 cooling was well underway through much of the belt by the end of the Cambrian (Alessio et al.,
659 2019b; Vincent et al., 2026).

660

661 **THE SOUTHEAST BRANCH OF THE EAST AFRICAN OROGEN**

662 ***South India, Sri Lanka, East Antarctica***

663 Southern India has been divided into a series of tectonic units with distinct protolith origins and
664 tectonothermal histories. From north to south these are: the Salem Block (sometimes called the
665 Northern Granulite Terrane); the Palghat-Cauvery shear system (“pcss” in Fig. 2); the Madurai
666 Block (“Mad” in Fig. 2); the Achancovil Zone (“asz” in Fig. 2); the Trivandrum Block (also known
667 as the Kerala Khondalite Belt); and the Nagercoil Block (both amalgamated as “TN” in Fig. 2) (e.g.
668 Santosh et al., 2009; Collins et al., 2014). The Palghat-Cauvery shear system has long been noted
669 to separate autochthonous parts of Neoproterozoic India from more exotic terranes to the south
670 (Bartlett et al., 1998; Cenko et al., 2004; Collins et al., 2014; Plavsa et al., 2015).

671

672 The northwest of the Madurai Block is composed of charnockite massifs with Sm–Nd and Rb–Sr
673 whole rock model ages in the range of 3170–2200 Ma (Bartlett et al., 1998; Bhaskar Rao et al.,
674 2003). U–Pb zircon ages from charnockites in this northwest Madurai Block have yielded a
675 consistent range of crystallisation ages between ca. 2.55 and 2.50 Ga (Ghosh et al., 2004; Brandt
676 et al., 2011; Plavsa et al., 2012). This northern region is separated from the rest of the
677 predominantly metasedimentary Madurai Block first by a lithological boundary that broadly
678 follows the Karur-Kamban-Painavu-Trichur lineament (known as the KKPT) (Ghosh et al., 2004)

679 that can also be seen as a zone of S-dipping reflectors in deep seismic surveys (Rajendra Prasad
680 et al., 2007). South of the KKPT (“kkpt” in Fig. 2) is a broad zone of highly deformed and
681 metamorphosed Archaean/Palaeoproterozoic metasedimentary rocks that continue until a line
682 approximately from Rajapalayam to Madurai (Plavsa et al., 2014; Kumar et al., 2017).
683 Neoproterozoic metasedimentary rocks with Mesoproterozoic to Neoproterozoic metaigneous
684 plutons that have continental arc-like chemistries dominate the region south of this
685 Rajapalayam–Madurai line and pass into the Achankovil Zone where Neoproterozoic rocks are
686 deformed into a prominent SE–NW striking high strain zone (Guru Rajesh and Chetty, 2006).

687
688 Some workers have subdivided the southern part of Kerala and Tamil Nadu into the Trivandrum
689 and Nagercoil Blocks (Santosh et al., 2003; Santosh et al., 2006). U–Pb zircon data from the
690 charnockites that are common in the region demonstrate that both blocks preserve similar ages
691 and really seem to be differentiated just on the dominance of charnockite in the Nagercoil Block
692 and metasedimentary rocks in the Trivandrum Block (Cenki et al., 2004; Kröner et al., 2012;
693 Johnson et al., 2015; Kumar et al., 2017; Clark et al., 2020). The metaigneous protoliths formed
694 at ca. 2040 Ma in an oceanic magmatic arc setting and are distinct from elsewhere in southern
695 India, but likely correlate with the basement of the Androyen and Anosyen terranes of southern
696 Madagascar (Tucker et al., 2014), possibly the Highland Complex of Sri Lanka (Kitano et al., 2018)
697 and even with parts of East Africa (Clark et al., 2020). The area including all these regions, with
698 the exception of East Africa, was named “SMIWH” (South Madagascar, India, Wannan-Highland
699 Complex) by Tucker et al. (2014), who argued that this terrane accreted to the Dharwar Craton
700 by the late Palaeoproterozoic. We note that this terrane is separated from the pre-1000 Ma crust
701 of India by the Neoproterozoic southern Madurai and Achankovil terranes (Plavsa et al., 2012;
702 Plavsa et al., 2015), which leads us to disagree with the proposed Palaeoproterozoic accretion
703 and suggest that this terrane combined with cratonic India during the Ediacaran high-grade
704 metamorphism seen throughout the region (Collins et al., 2007; Clark et al., 2009; Collins et al.,
705 2014; Taylor et al., 2014; Plavsa et al., 2015). We also point out that no reliable evidence exists
706 for pre-Stenian basement in the Sri Lankan Wannan Complex, and that it shouldn’t be considered
707 part of this terrane; the acronym SMIWH then is inaccurate.

708

709 We suggest that the contiguous Gondwanan terrane encompassing the Androyen/Anoyesen
710 domains of Madagascar, the Trivandrum Block of southmost India and the Highland Complex of
711 Sri Lanka be called 'Pandya' after i) the named used for the metamorphic belt of southern India
712 (Pandyan Mobile Belt, Ramakrishnan, 1993), ii) the ancient Tamil dynasty of southern India,
713 whose lands encompassed parts of Sri Lanka at their greatest extent.

714

715 **DISCUSSION**

716 ***The Plate Tectonic Evolution of the East African Orogen***

717 The tectonic geography represented by the various terranes of the East African Orogen can be
718 difficult to deduce where extreme metamorphism and deformation has transposed all physical
719 evidence and often rendered geochemical evidence enigmatic. Such obfuscation is a particular
720 challenge in the southern East African Orogen—a region known as the Mozambique Belt (Fritz et
721 al., 2013). Along orogenic strike, though, outcrop metamorphic grade decreases towards the
722 north—from granulite and upper amphibolite grade rocks in the southern EAO to greenschist
723 facies and sub-greenschist facies rocks preserved in the northern parts of the EAO . By
724 comparison, in the northern EAO most surface rocks experienced metamorphism of no more
725 than greenschist-facies and original sedimentary/volcanic features are commonly preserved as
726 are near-original chemistries of the rocks. It is here in the Arabian-Nubian Shield where many
727 pre-continent/continent collision tectonic events that affected the region can be best defined
728 (Johnson et al., 2011; Collins et al., 2021a; Collins et al., 2021b).

729

730 ***The East African Orogen—the Largest Mountain Belt of the Last Billion Years?***

731 There is a good case to suggest that the EAO is the largest collisional orogen of the last billion
732 years simply based on its footprint on a reconstructed Gondwana. Extending across
733 approximately 100 degrees of longitude at low to moderate southern latitudes (Collins et al.,
734 2021b) the orogen was over 10,000 kms long and extend over 1000 km at its widest point (in the
735 region now preserved in Mozambique, Madagascar and Southern India)(Figs. 1, 2). The scale is
736 comparable to the modern Alpine-Himalaya chain, and like this modern orogen, the EAO was

737 large enough to strongly change the oceanic radiogenic strontium isotopic curve (Chen et al.,
738 2022). In fact, global ocean $^{87}\text{Sr}/^{86}\text{Sr}$ values only rise dramatically twice in the last billion years;
739 once from 50 Ma to present, due to erosion of the growing Himalaya, and in the late
740 Neoproterozoic (Chen et al., 2022). Zhu et al. (2022) looked at the scale of orogens through time
741 from a different perspective. By examining the rare earth element chemistry of dated detrital
742 zircons, they showed that there are two main times of 'supermountain' formation, one in the
743 Palaeoproterozoic and a second contemporaneous with the EAO. The youth of the Himalayan
744 orogen is the likely reason for no significant record of it in these detrital zircons. Therefore, as
745 well as the EAO (along with contemporaneous Gondwana-forming orogens in Africa and South
746 America) being of a scale to affect ocean water composition, it also thickened the crust enough
747 to significantly affect the trace-element chemistry of zircon-producing magmas. This suggests
748 that the orogen was not only spatially extensive, but also formed mountains of an elevation at
749 least as high as those seen in Asia today. As proposed by Zhu et al. (2022), erosion of this
750 'supermountain' would likely stimulate biological productivity and widely effect the wider
751 planetary system (e.g., Squire et al., 2006; Halverson et al., 2010). The orogen's broad E-W
752 orientation and location in relatively low to moderate latitudes likely accentuated its erosion and
753 multiplied its effect on other Earth systems (in a similar manner to the Late Palaeozoic orogens
754 demonstrated by Godderis et al., 2017). Merdith et al. (Submitted) demonstrated the importance
755 of this within a computational whole-Earth, where they traced the evolution of tectonic plate
756 boundaries, to automatically isolate specific tectonic environments that are associated with
757 mountain building, such as continental arcs, continental collisions, rifts and large igneous
758 provinces. From this they simulated orogenic growth, and erosion, over the last 1 Ga, using
759 parameters and limits derived from the present-day expression of topography on Earth to
760 provide a quantitative and tractable basis for palaeoclimate or landscape evolution modelling
761 over the last 1 Ga. This semi-automated topography model uses 'rules' relating orogenic
762 topography to the nature and location of plate boundaries. The next step is to use geological data
763 to constrain topographic evolution directly from nature.
764

765 To obtain a better understanding of the role the EAO plays in the tumultuous changes to the
766 climate, biosphere and atmosphere in the Neoproterozoic an understanding of the spatial and
767 temporal evolution of elevation through the orogen is needed. Unravelling topography from the
768 now denuded and dispersed remains of the East African Orogen mountains is a complex task. We
769 have taken the approach here of mapping pressure and time determinations from the literature
770 on a reconstruction of Gondwana (Merdith et al., 2021). We limit our analyses to exclude low
771 geothermal gradient metamorphism (< 450 K/GPa) as this is usually interpreted as subduction-
772 zone related (Brown and Johnson, 2019). In this situation, pressure (depth) will not necessarily
773 relate to surface elevation due to the non-isostatic nature of these environments. We have also
774 ignored the possible effects of differential stress (Schmalholz and Podladchikov, 2014;
775 Tajčmanová et al., 2021; Zuza et al., 2022) due to the difficulty of quantifying its effect on mean
776 stress, metamorphic determinations (pressure).

777

778 A simple isostatic correction to present day elevation can be produced from metamorphic
779 pressure estimates to estimate palaeo-elevation (Fig. 3). Given a peak metamorphic pressure,
780 P_s , at the time of metamorphism, the height of eroded material, h , can be estimated from an
781 assumed density (2850 kg m^{-3}) for the eroded material, ρ , and gravity, g , by

$$782 \quad h = \frac{P_s}{\rho g}.$$

783 Assuming the lower crust and mantle lithosphere at the time of metamorphism is the same
784 today, their contributions cancel out of the isostatic balance; thus mantle density, ρ_m , and
785 present day elevation, ε_{pd} are the only additional parameters needed to compute the elevation
786 at the time of peak metamorphism, ε_{EAO} . Using the local isostatic balance equations: (1) $\rho h =$
787 $\rho_m h_m$ and (2) $h = h_m + \varepsilon_{EAO} - \varepsilon_{pd}$, where h_m is the thickness of mantle needed to compensate
788 the change in load, we estimate the palaeo-elevation by,

$$789 \quad \varepsilon_{EAO} = \varepsilon_{pd} + \frac{P_s}{\rho g} \left(1 - \frac{\rho}{\rho_m} \right).$$

790

791 A total of 197 metamorphic conditions have been compiled (Table 1), supplementing the P–T
792 database by Brown and Johnson (2019). Present-day elevation was determined by averaging
793 pixels in a 25 km radius about the sample location, though in many cases locations are

794 approximated from a map or description. While it is beyond the scope of this study to produce
795 a rigorous elevation model, which ideally would incorporate thermal effects and compositional
796 uncertainties (Hasterok and Chapman, 2007), where pressure ranges have been provided an
797 elevation range was computed (Table 1).

798
799 Predicted elevations range from near sea-level to a maximum of ca. 10 km, with an average of
800 5.1 ± 1.6 km, similar in elevation to the modern Tibetan Plateau, and over a similar area (Figs. 1,
801 5). The modelled EAO palaeo-elevations are greater than the global average palaeo-elevations
802 (Fig. 4) and are normally distributed. One may expect a more exponential distribution for
803 elevation, though it is unsurprising that elevation predicted from peak metamorphic pressures
804 does not. The primary reason for this difference is the lack of precise recording of pressures at
805 low metamorphic grades, which are difficult due to kinetic rates at low temperatures. Hence our
806 estimates likely yield elevation estimates in the orogenic plateau and range crest (Fig. 5). Since
807 there is no obvious decrease in elevation at the eastern and western edges of the plateau, the
808 area of elevated terrain is likely much greater than the distribution of model estimates.

809
810 Based on these simple elevation estimates, we suggest that the high topography varied spatially
811 in time as the orogen evolved. High elevations were created in the first phase of the orogen
812 (680–640 Ma; i.e. the East African Orogeny of Collins and Pisarevsky, 2005), recorded as high
813 elevations > 6 km in the Tanzanian Eastern Granulites associated with shortening during
814 subduction and collision of Azania with the Congo-Tanzania-Bangweulu Block (Fig. 5). In the
815 second phase (640–580 Ma), the elevation remained high in the Mozambique Belt and southern
816 Azania. At this time, many regions in the Arabian-Nubian Shield also reached peak metamorphic
817 pressure conditions, though at lower maxima that result in a lower topography (~ 2.5 –4 km, Fig.
818 5 and Table 1). The final stage of the EAO (The Malagasy Orogeny of Collins and Pisarevsky, 2005)
819 resulted in the development of an extensive orogenic plateau, with the highest modelled
820 elevations (8–10 km) in the south, in present-day coastal East Antarctica, and throughout a broad
821 plateau that extended from the margin of the Congo–Tanzania–Bangweulu continent, across
822 Azania in present-day Madagascar, Sri Lanka and the Southern Granulite Terrane of India (Figs.

823 1, 2, 5). It is unlikely that the highest elevations are accurate as regional compensation would
824 likely have resulted in lower elevations, however, we assert that the aerial extent of the high
825 elevations in the plateau regions is reasonable, i.e., within the bounds of elevation observed in
826 Tibet and the Himalaya today (Fig. 4). On the basis of these estimates, we suggest that the EAO
827 was amongst the largest, highest mountain belts known on Earth, rivalling the Alpine-Himalayan
828 Orogen of today and lending support to hypotheses that have the orogen fundamental to earth
829 surface systems tipping points, such as facilitating carbon burial and planetary oxygenation that
830 are broadly coeval with the orogen's apogee (e.g., Zhu et al., 2022).

831

832 ***Suggestions for further work***

833

834 A grand challenge of earth science is to be able to map the evolution of Earth's surface systems
835 through its history. This is a herculean task, but a worthy task, as it is only by developing a deeper
836 understanding of the geological record that can drive more naturalistic models of the planet that
837 we can understand how our planet works, and how the geosphere interacts with the atmosphere
838 to develop the climate, hydrosphere and biosphere (e.g., Mills et al., 2025). Developing a model
839 of the Earth system over the ca. 500 million years of the Neoproterozoic involves reconstructing
840 both the plate tectonic evolution of the planet, and the evolution of the planet's surface
841 elevation.

842

843 The reconstruction presented here (Figs. 1, 2), and the palaeo-geographically controlled palaeo-
844 elevation estimates (Fig. 5), are only the first attempt at integrating the full plate tectonic record
845 with the metamorphic record to track the evolution of this one (albeit large) mountain range.
846 Much of the geology of the East African Orogen is poorly known, especially when compared with
847 that of Phanerozoic mountain ranges such as the European Alps, North American Appalachians
848 or Chinese Qinling mountains. Much work is needed to unravel the paleo-plate tectonic evolution
849 of the orogen, especially in the countries of east and northeast Africa, Arabia, Madagascar, South
850 Asia and East Antarctica. This is in addition to the other Neoproterozoic orogens that lace South
851 America, Australia and parts of Asia.

852

853 We hope to have demonstrated that when triaged carefully, the metamorphic record preserves
854 palaeo-topographic information that is difficult to recover by other methods. We note that much
855 of the available metamorphic record through Proterozoic orogens is governed by point analyses
856 on restricted outcrops where high variance lithologies occur that are used to constrain the
857 pressure-temperature and time evolution of that one location. We encourage future pressure-
858 time campaign-style studies that may be able to determine the geometry of orogenic topography
859 and along-strike variations that will considerably improve the resulting models.

860

861 As an example of what is possible. We undertook a reconnaissance pressure-time study of
862 southern India that was reported in Collins et al. (2022b). Here we dated garnets using the in-situ
863 Lu-Hf technique over an orogenic transect (Tamblyn et al., 2022) and examined the trapped
864 pressures of quartz inclusions using RAMAN spectroscopy to obtain peak pressures. Many
865 exhumed orogens are garnet-rich and a similar approach could be done through many of the
866 Proterozoic orogens to better understand their topographic evolution.

867

868 The answer in the end involves a community-wide approach to supporting geological research
869 globally, and especially in the global south. Then integrating plate-tectonic reconstructions
870 developed from these works into a global reconstruction. Topography can then be added by
871 combining estimates of past elevation from the proximity of a region to a plate boundary (in the
872 style of Merdith et al., Submitted) with estimates from geochemistry of igneous rocks (e.g. Zhu
873 et al., 2022; Zhou et al., 2025) and estimates from the metamorphic record as discussed here.

874

875 **CONCLUSIONS**

876 The East African Orogen is one of the largest known orogens on the planet, on a similar, or greater
877 scale, than the present-day Alpine-Himalaya Orogen. Reconstructions of the East African Orogen
878 show that it not only bisected Gondwana, but it also developed a thick orogenic plateau that
879 rivals Tibet for elevation and area (Fig. 1). The East African Orogen evolved from a
880 Mesoproterozoic accretionary orogen that developed to the east of the West African Craton and

881 north of the Congo-Tanzania-Bangweulu Block. Throughout the Tonian, accretionary orogenesis
882 characterized the orogen and volcanic arcs developed on the margins of the growing nuclei of
883 Africa (soon to be central Gondwana) and within the Mozambique Ocean. The collision of Azania
884 (and other intra-Mozambique Ocean continents) with the active margin of Africa caused an early
885 continent-continent collisional orogeny—the East African Orogeny. This was later followed by
886 the Ediacaran collision of Neoproterozoic India with the growing kernel of central Gondwana.

887
888 The available metamorphic record supports the designation of the East African Orogen as, if not
889 the largest, then one of the largest mountain ranges in Earth history (Fig. 4). Past ground-
890 elevation estimates constructed from the triaged metamorphic record are located on the full-
891 plate tectonic reconstruction of Cao et al. (2024), which is fundamentally based on Merdith et al.
892 (2021), and reveals the elevation consequences of the series of plate-tectonic events (Fig. 4). This
893 also demonstrates the along-strike variability along the orogen, with contemporary palaeo-
894 elevations in the Arabian-Nubian Shield region being considerably lower than in the Mozambique
895 Belt, reflecting the geometry and kinematics of the plate-movements at the time. Our plate-
896 tectonic/palaeo-elevation approach is suggested as a way forward in reconstructing the shape of
897 the Earth in deep time—a key parameter in future earth systems models of the planet.

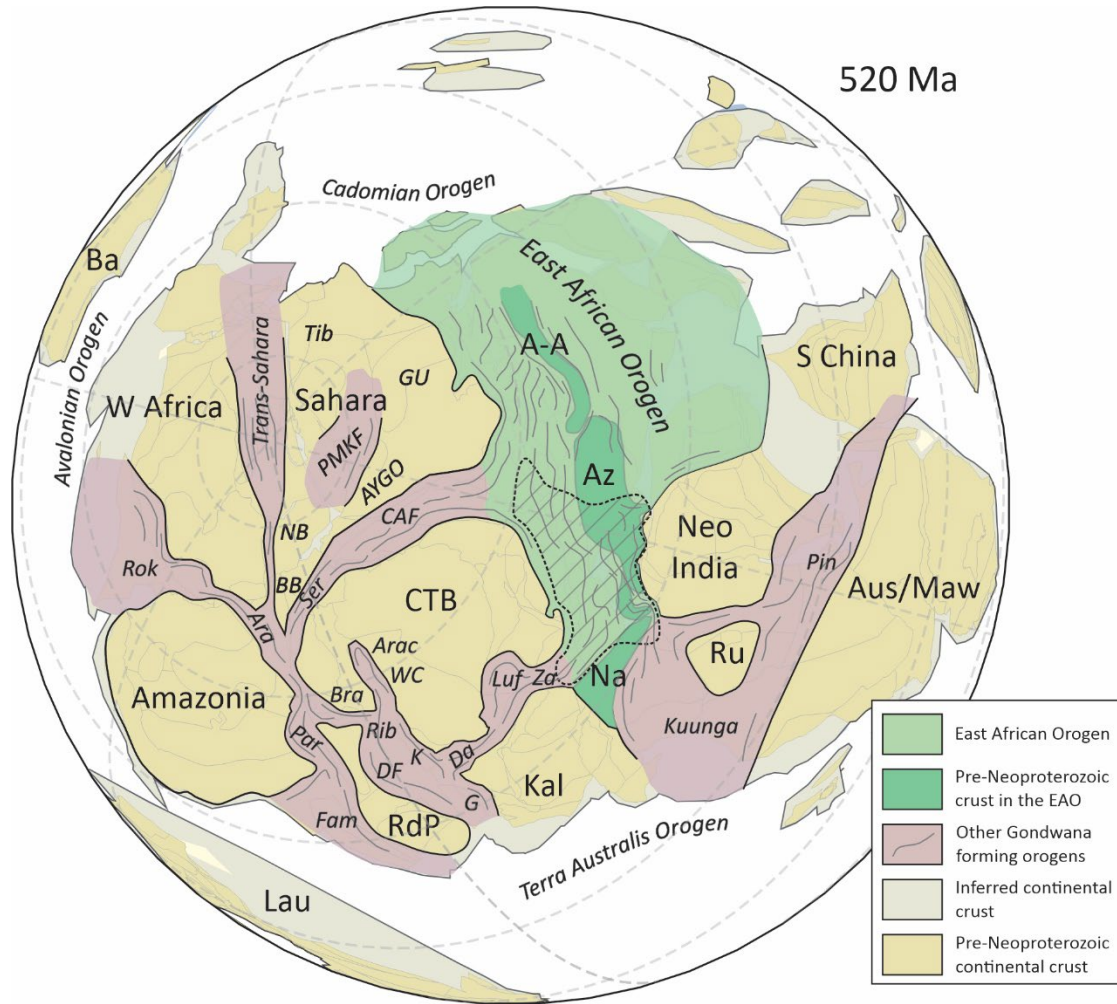
898
899 **ACKNOWLEDGMENTS**
900 ASC and MLB are funded by Australian Research Council grants FL240100114 and DP250102570.
901 ASM is funded by DE230101642. ASC thanks the numerous colleagues and students who have
902 assisted on the projects that led to his fascination with the East African Orogen and the formation
903 of Gondwana.

904

905
906 **Table 1 - Peak metamorphic conditions and model palaeo elevations within the East African Orogen.**
907 **(see spreadsheet).**

908

909 **FIGURE CAPTIONS**



910

911

912 Figure 1: Reconstruction of Gondwana in the early Cambrian (520 Ma), after Merdith et al. (2021)

913 with the East African Orogen (EAO) outlined along with major regions of Pre-Neoproterozoic

914 crust reworked within the EAO; A-A = Afif-Abas Terrane, Az = Azania, Na = Nampula Terrane.

915 Other major Gondwana-forming orogens are outlined, which are; Ara = Araguaia Belt, Arac =

916 Aracuaí Orogen, Bra = Brasília Belt, CAF = Central African Fold Belt, Da = central Damara Belt, DF

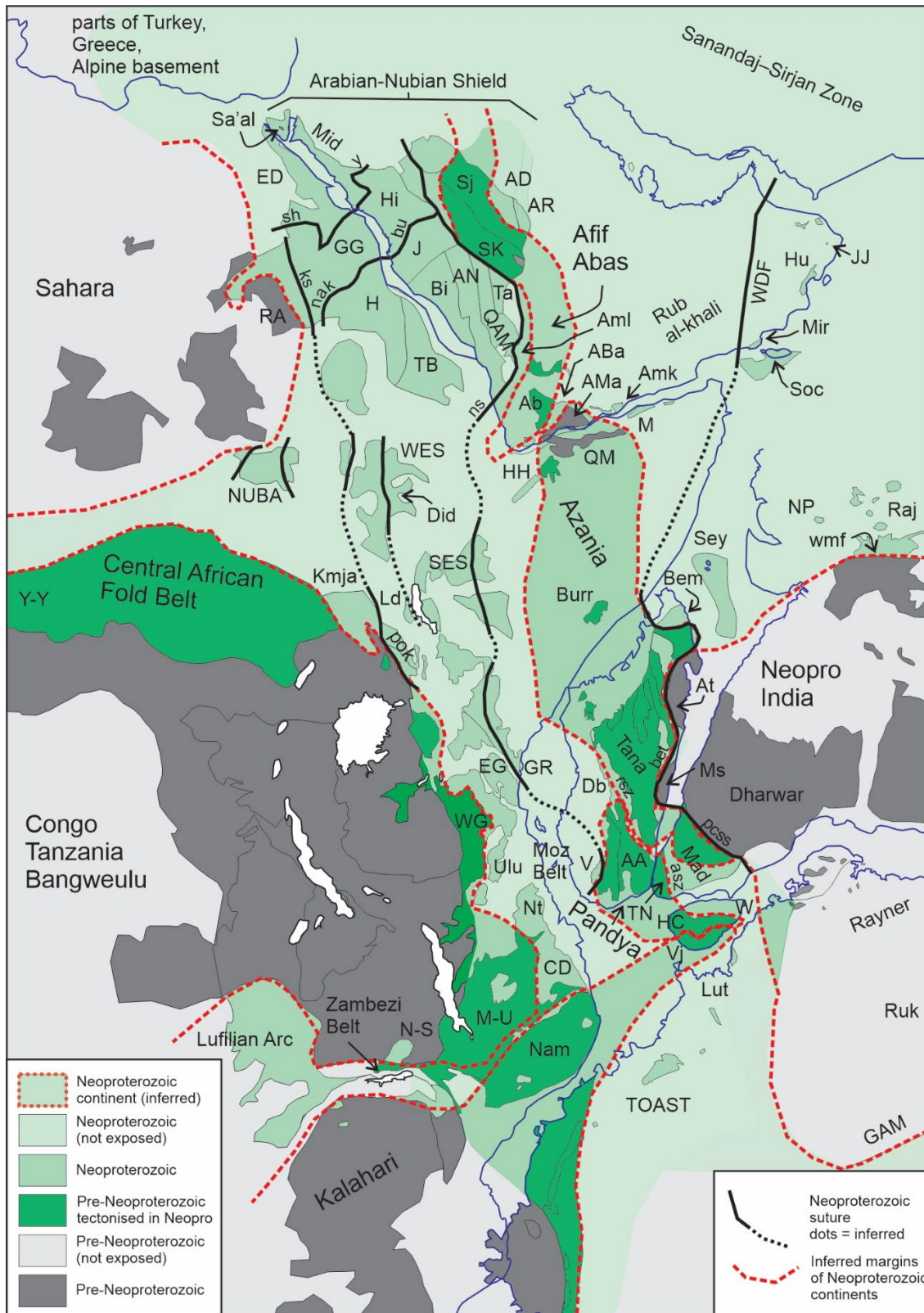
917 = Dom Feliciano Belt, Fam = Famatinian Orogen, G = Gariep Belt, K = Kaoko Belt, Kuunga = Kuunga

918 Orogen, Luf = Lufilian Arc, Par = Paraguay Belt, PMKF = Poli-Mayo Kebbi-Lake Fitri Terrane, Pin =

919 Pinjarra Orogen, Rib = Ribeira Belt, Rok = Rokelide Orogen, Ser = Sergipano Orogen, Trans-Sahara

920 = Trans-Saharan Orogen, WC = West Congo Orogen, Za = Zambezi Belt. The major Neoproterozoic

921 continental blocks are; Aus/Maw = Australia/Mawson Continent, Ba = Baltica, CTB = Congo-
922 Tanzania-Bangweulu (also includes the São Francisco craton of Brazil), Kal = Kalahari, Lau =
923 Laurentia, Neo India = Neoproterozoic India, W Africa = West Africa (including the São Luis Block
924 of Brazil), RdP = Río de la Plata (and including the putative Paranapanema craton), Ru = Ruker
925 Terrane (likely a continuation of Neoproterozoic India), Sahara = Saharan basement (including
926 the Nigeria-Benin block [NB], the Brazilian Borborema Province [BB], Tibesti [Tib], Gebel Uweinat
927 [GU] and the Adamawa-Yadé-Guéra-Ouaddaï Terrane [AYGO]), S China = South China. The broad
928 sites where three of the Gondwana-peripheral orogens will form are also marked, these are the
929 Avalonian Orogen, the Cadomian Orogen, and the Terra Australia Orogen. The cross-hatched
930 zone in the EAO is where the highest-grade metamorphic rocks from the East African orogen and
931 Malagasy orogens are found, which approximates to the position of the Mozambique Belt and
932 forms the past position of the large orogenic plateau discussed in this paper. Broad orogenic
933 strike lines are added within the Gondwana-forming orogens.



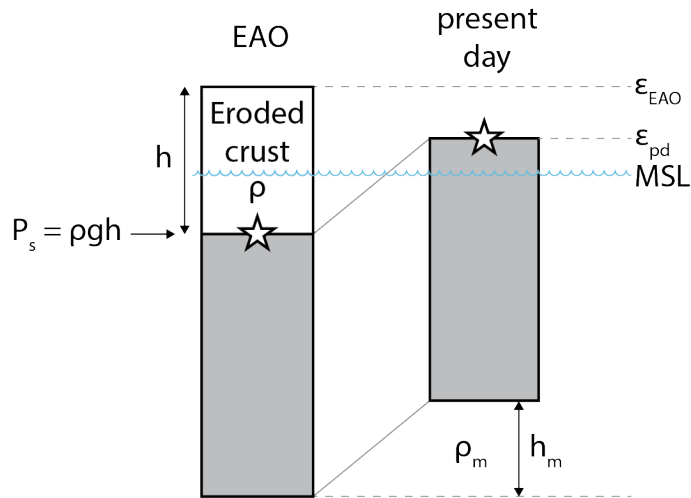
934

935 Figure 2: Reconstruction of Central Gondwana at 550 Ma (using the GPlates reconstruction of

936 Merdith et al. 2021 as the basemap). Crust that was significantly deformed and metamorphosed

937 (tectonised) in the Neoproterozoic, or formed in the Neoproterozoic, are coloured shades of
938 green. Abbreviations used are: AA = Anosyen-Andasibe domains, Ab = Abas Terrane, ABa = Al
939 Bayda Terrane, AD = Ad Dawadmi Terrane, AMa = Al Mafid Terrane, Amk = Al Mukalla Terrane,
940 Aml = Amlah Terrane, AN = An Nimas Terrane, AR = Ar Rayn Terrane, At = Antongil Domain, Bem
941 = Bemarivo Belt (the Bobakindro terrane is the northernmost part of this belt), Bi = Bidah Terrane,
942 CD = Cabo Delgado Complex, Db = Dabolava Suite (arc), Did = Didesa Terrane, ED = Eastern Desert
943 of Egypt, EG = Eastern Granulites, GG = Gabgaba/Gebeit Terrane, GR = Galana River, H = Haya
944 Terrane, HC = Highland Complex, HH = Harar-Hirna, Hi = Hijaz Terrane, Hu = Huqf, J = Jiddah
945 Terrane, JJ = Jebel Ja'alan, Kmja = Karamoja Belt, Ld = Lodwar, Lut = Lutzöw-Holm Bay, M = Maydh
946 (or Mait) Complex, Mad = Madurai Block, Mid = Midyan Terrane, Mir = Mirbat, Ms = Masora
947 Domain, M-U = Marrupa-Unango complexes, Nam = Nampula Complex, NP = Nanga Parkar, N-S
948 = Nyimba-Sinda Terrane, Nt = Ntaka Terrane, NUBA = Nuba Mountains, QAM = Al Qarah-Malahah
949 Terrane, QM = Qabri Bahar and Mora complexes, RA = Rahaba-Absol Terrane, Raj = Rajasthan,
950 Ray = Rayner Complex, Ruk = Ruker Domain, Sa'al = Sa'al Metamorphic Complex, Sahara =
951 Sarahan basement (including pre-Neoproterozoic crustal terranes and Neoproterozoic juvenile
952 terranes), SES = Southern Ethiopian Shield, Sey = Seychelles, Sj = Suwaj, SK = Siham-Khida Terrane,
953 Soc = Socotra, Ta = Tathlith Terrane, Tana = Antananarivo Domain, TB = Tokar/Barka Terrane, TN
954 = Trivandrum-Nagercoil blocks, Ulu = Uluguru Mountains, V = Vohibory Domain, Vj = Vijayan
955 Complex, W = Wannu Complex, WES = Western Ethiopian Shield, WG = Western Granulites, Y-Y
956 Yaoundé-Yangana nappes. Shear zones and sutures are marked with the following acronyms; asz
957 = Achancovil Shear Zone, bet = Betsimisaraka Suture (in the Anaboriana-Manampotsy belt), bu =
958 Bi'r Umq Suture, kkpt = Karur-Kamban-Painavu-Trichur Lineament, ks = Keraf Suture, nak =
959 Nakasib Suture, ns = Nabitah Suture, pok = West Pokat Suture, pcss = Palghat-Cauvery Shear
960 System, rsz = Ranotsara Shear Zone, sh = Sol-Hamed Suture, wmf = Western Margin Fault, y =
961 Yanbo Suture.

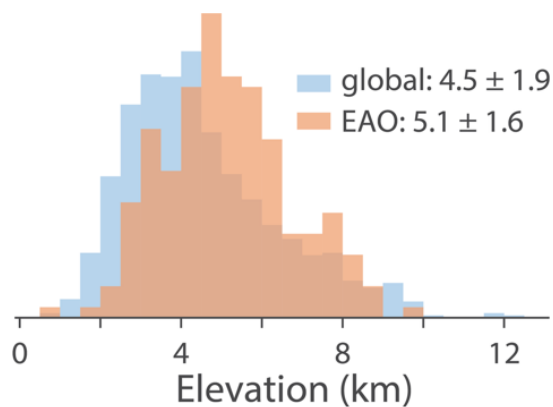
962



963

964 Figure 3: Isostatic columns used to estimate elevation during the East African Orogen from
 965 metamorphic pressure estimates. Isostatic column during the East African Orogen (left) included
 966 overburden that eroded (average density, ρ , and thickness, h), exposing the metamorphic
 967 pressure (P_s , star) at present day (right).

968

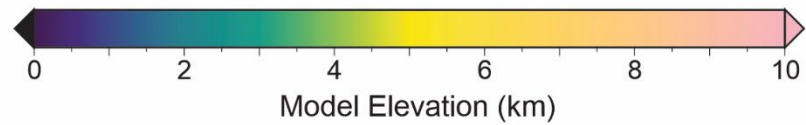
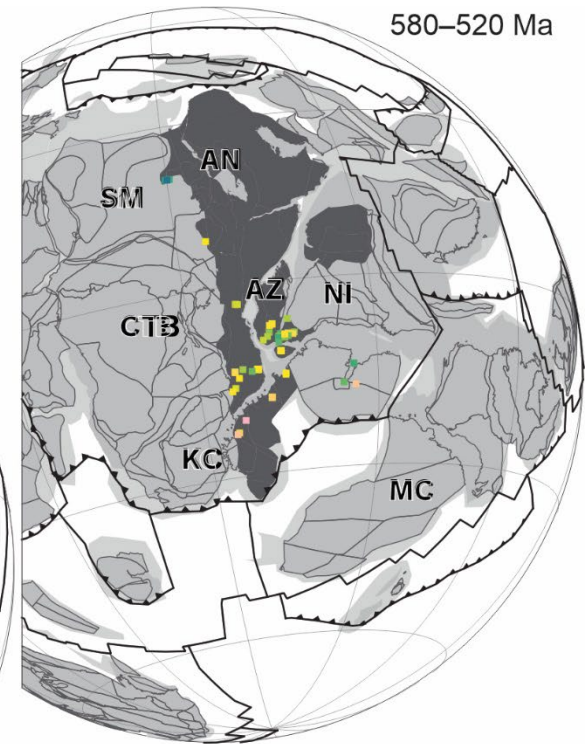
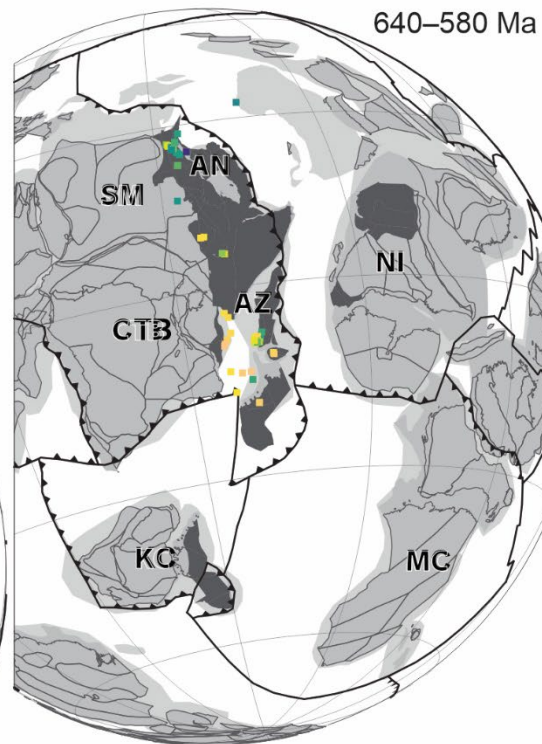
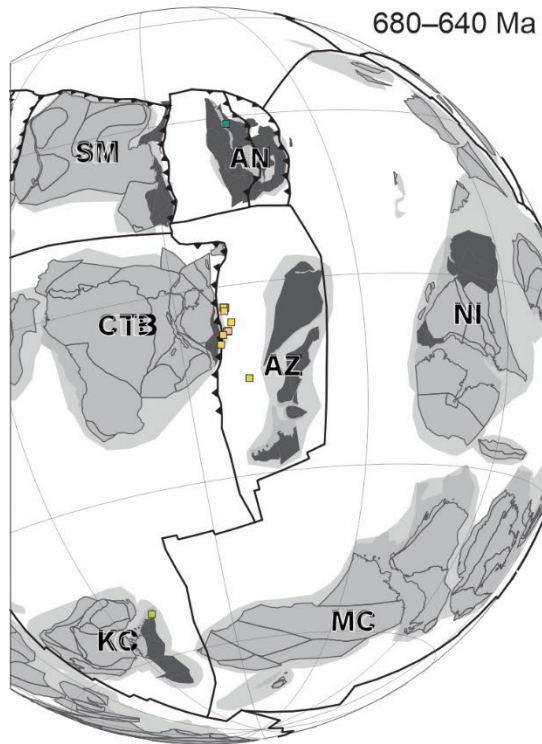


969

970 Figure 4: Palaeo-elevation estimates for the East African Orogen (EAO) compared to the global
 971 dataset excluding EAO data. Individual palaeo-elevation estimates are provided in Table 1. The
 972 global estimates are derived from pressures included in an expanded metamorphic database,
 973 originally by Brown and Johnson (2019). Data were prefiltered for metamorphic pressures below
 974 2 GPa and metamorphic thermal gradients above 450 K/GPa to remove most subduction-related
 975 events.

976

- AN - Arabian-Nubian Shield
- AZ - Azania
- CTB - Congo–Tanzania–Bangweulu
Continent
- KC - Kalahari Continent
- MC - Australia/Mawson Continent
- NI - Neoproterozoic India
- S - Saharan basement



978 Figure 5: Palaeo-elevation estimates for the East African Orogen. The P–T locations have been
979 reconstructed from the tectonic model by Cao et al. (2024) at time steps 660 Ma, 600 Ma, and
980 550 Ma, corresponding to the palaeo-elevation estimates at 680–640 Ma, 640–580 Ma, and 580–
981 520 Ma, respectively. The plate models are fixed relative to the Congo-Tanzania-Bangweulu
982 Continent (CTB).

983

984 REFERENCES CITED

985

- 986 Abdelsalam, M.G. and Dawoud, A.S., 1991. The Kabus ophiolitic melange, Sudan, and its
987 bearing on the western boundary of the Nubian Shield. *Journal of the Geological Society*,
988 London, 148: 83-92.
- 989 Abdelsalam, M.G., Liegeois, J.P. and Stern, R.J., 2002. The Saharan Metacraton. *Journal of*
990 *African Earth Sciences*, 34(3-4): 119-136.
- 991 Abdelsalam, M.G. and Stern, R.J., 1996. Sutures and shear zones in the Arabian-Nubian Shield.
992 *Journal Of African Earth Sciences*, 23(3): 289-310.
- 993 Abdelsalam, M.G., Stern, R.J., Copeland, P., El-Faki, E.-F.M., Al-Hur, B. and Ibrahim, F.M.,
994 1998. The Neoproterozoic Keraf Suture in NE Sudan: sinistral transpression along the
995 eastern margin of West Gondwana. *Journal of Geology*, 106: 133-147.
- 996 Abdelsalam, M.G., Stern, R.J., Schandelmeier, H. and Sultan, M., 1995. Deformation history of
997 the Keraf Zone in NE Sudan, revealed by Shuttle Imaging Radar. *Journal of Geology*,
998 103: 475–491.
- 999 Abebe, E., Alene, M., Tesfaw, B., Sano, T. and Kusaba, Y., 2025. Structural and metamorphic
1000 evolution of Neoproterozoic rocks in Bensa-Girja area, southern Ethiopia. *Journal of*
1001 *African Earth Sciences*, 230.
- 1002 Al-Barwani, B. and McClay, K., 2008. Salt tectonics in the Thumrait area, in the southern part of
1003 the South Oman Salt Basin: Implications for mini-basin evolution. *Georabia*, 13: 77-
1004 108.
- 1005 Al-Lazki, A., Ebinger, C., Kendall, M., Helffrich, G., Leroy, S., Tiberi, C., Stuart, G. and Al-
1006 Toobi, K., 2012. Upper mantle anisotropy of southeast Arabia passive margin [Gulf of
1007 Aden northern conjugate margin], Oman. *Arabian Journal of Geosciences*, 5(5): 925-934.
- 1008 Al Rawahi, H., Gómez-Pérez, I., Bergmann, K.D., McCabe, R. and Cantine, M.D., 2026. Syn-
1009 tectonic deposition during final closure of the Mozambique Ocean: the Ediacaran Fara
1010 Formation in northern Oman. *Precambrian Research*, 442: 108095.
- 1011 Alessio, B.L., Blades, M.L., Murray, G., Thorpe, B., Collins, A.S., Kelsey, D.E., Foden, J.,
1012 Payne, J., Al-Khribash, S. and Jourdan, F., 2018. Origin and tectonic evolution of the NE
1013 basement of Oman: a window into the Neoproterozoic accretionary growth of India?
1014 *Geological Magazine*, 155(5): 1150-1174.
- 1015 Alessio, B.L., Collins, A.S., Siegfried, P., Glorie, S., De Waele, B., Payne, J. and Archibald,
1016 D.B., 2019a. Neoproterozoic tectonic geography of the south-east Congo Craton in
1017 Zambia as deduced from the age and composition of detrital zircons. *Geoscience*
1018 *Frontiers*, 10(6): 2045-2061.

- 1019 Alessio, B.L., Glorie, S., Collins, A.S., Jourdan, F., Jepson, G., Nixon, A., Siegfried, P.R. and
1020 Clark, C., 2019b. The thermo-tectonic evolution of the southern Congo Craton margin as
1021 determined from apatite and muscovite thermochronology. *Tectonophysics*, 766: 398-
1022 415.
- 1023 Allen, P.A., 2007. The Huqf Supergroup of Oman: Basin development and context for
1024 Neoproterozoic glaciation. *Earth Science Reviews*, 84: 139-185.
- 1025 Anders, B., Reischmann, T., Kostopoulos, D. and Poller, U., 2006. The oldest rocks of Greece:
1026 first evidence for a Precambrian terrane within the Pelagonian Zone. *Geological*
1027 *Magazine*, 143(1): 41-58.
- 1028 Andersson, U.B., Ghebreab, W. and Teklay, A., 2006. Crustal evolution and metamorphism in
1029 east-central Eritrea, south-east Arabian-Nubian Shield. *Journal of African Earth Sciences*,
1030 44(1): 45-65.
- 1031 Antonio, P.Y.J., Rouse, S., Macouin, M., Ganerod, M., Roques, D., Denèle, Y. and Benoit, M.,
1032 2026. East side story of Gondwana: the last frontier of the Arabian Nubian shield at 720
1033 Ma based on new high-quality paleomagnetic pole. *Gondwana Research*, 149: 113-126.
- 1034 Apen, F.E., Rudnick, R.L., Cottle, J.M., Kylander-Clark, A.R.C., Blondes, M.S., Piccoli, P.M.
1035 and Seward, G., 2020. Four-dimensional thermal evolution of the East African Orogen:
1036 accessory phase petrochronology of crustal profiles through the Tanzanian Craton and
1037 Mozambique Belt, northeastern Tanzania. *Contributions to Mineralogy and Petrology*,
1038 175(11).
- 1039 Appel, P., Möller, P. and Schenk, V., 1998. High-pressure granulite facies metamorphism in the
1040 Pan-African belt of eastern Tanzania: P-T-t evidence against granulite formation by
1041 continent collision. *Journal of Metamorphic Geology*, 16: 491-509.
- 1042 Arboit, F., Ceriani, A., Collins, A., Hennhofer, D., Pilia, S. and Decarlis, A., 2024. The tectonic
1043 setting of the late Ediacaran eastern Arabian basement (ca. 550 Ma): New
1044 geochronological and geochemical constraints from the basements of Oman and the
1045 United Arab Emirates. *Gondwana Research*, 130: 203-219.
- 1046 Archibald, D.B., Collins, A.S., Armistead, S.E., Foden, J.D., Payne, J.L. and Razakamanana, T.,
1047 2023. Zircon U–Pb, oxygen, and hafnium isotopic characteristics of the Neoproterozoic–
1048 Palaeoproterozoic Betsiboka Suite, Madagascar: tracing source to sink pathways in
1049 Proterozoic and Phanerozoic provenance studies. *Geological Society, London, Special*
1050 *Publications*, 531(1): SP531-2022-162.
- 1051 Archibald, D.B., Collins, A.S., Foden, J.D., Payne, J.L., Holden, P., Razakamanana, T., De
1052 Waele, B., Thomas, R.J. and Pitfield, P.E.J., 2016. Genesis of the Tonian Imorona-
1053 Itsindro magmatic Suite in central Madagascar: Insights from U-Pb, oxygen and hafnium
1054 isotopes in zircon. *Precambrian Research*, 281: 312-337.
- 1055 Archibald, D.B., Collins, A.S., Foden, J.D., Payne, J.L., Macey, P.H., Holden, P. and
1056 Razakamanana, T., 2018. Stenian-Tonian arc magmatism in west-central Madagascar: the
1057 genesis of the Dabolava Suite. *Journal of the Geological Society*, 175(1): 111-129.
- 1058 Archibald, D.B., Collins, A.S., Foden, J.D., Payne, J.L., Taylor, R., Holden, P., Razakamanana,
1059 T. and Clark, C., 2015. Towards unravelling the Mozambique Ocean conundrum using a
1060 triumvirate of zircon isotopic proxies on the Ambatolampy Group, central Madagascar.
1061 *Tectonophysics*, 662: 167-182.
- 1062 Archibald, D.B., Collins, A.S., Foden, J.D. and Razakamanana, T., 2017. Tonian Arc
1063 Magmatism in Central Madagascar: The Petrogenesis of the Imorona-Itsindro Suite.
1064 *Journal of Geology*, 125(3): 271-297.

1065 Armistead, S.E., Collins, A.S., Merdith, A.S., Payne, J.L., Cox, G.M., Foden, J.D.,
1066 Razakamanana, T. and De Waele, B., 2019. Evolving Marginal Terranes During
1067 Neoproterozoic Supercontinent Reorganization: Constraints From the Bemarivo Domain
1068 in Northern Madagascar. *Tectonics*, 38(6): 2019-2035.

1069 Armistead, S.E., Collins, A.S., Payne, J.L., Foden, J.D., De Waele, B., Shaji, E. and Santosh, M.,
1070 2018. A re-evaluation of the Kumta Suture in western peninsular India and its extension
1071 into Madagascar. *Journal of Asian Earth Sciences*, 157: 317-328.

1072 Armistead, S.E., Collins, A.S., Schmitt, R.S., Costa, R.L., De Waele, B., Razakamanana, T.,
1073 Payne, J.L. and Foden, J.D., 2021. Proterozoic Basin Evolution and Tectonic Geography
1074 of Madagascar: Implications for an East Africa Connection During the Paleoproterozoic.
1075 *Tectonics*, 40(3): e2020TC006498.

1076 Ashwal, L.D., Armstrong, R.A., Roberts, R.J., Schmitz, M.D., Corfu, F., Hetherington, C.J.,
1077 Burke, K. and Gerber, M., 2007. Geochronology of zircon megacrysts from nepheline-
1078 bearing gneisses as constraints on tectonic setting: implications for resetting of the U-Pb
1079 and Lu-Hf isotopic systems. *Contributions to Mineralogy and Petrology*, 153(4): 389-
1080 403.

1081 Ashwal, L.D., Solanki, A.M., Pandit, M.K., Corfu, F., Hendriks, B.W.H., Burke, K. and Torsvik,
1082 T.H., 2013. Geochronology and geochemistry of Neoproterozoic Mt. Abu granitoids, NW
1083 India: Regional correlation and implications for Rodinia paleogeography. *Precambrian
1084 Research*, 236: 265-281.

1085 Bartlett, J.M., Dougherty-Page, J.S., Harris, N.B.W., Hawkesworth, C.J. and Santosh, M., 1998.
1086 The application of single zircon evaporation and model Nd ages to the interpretation of
1087 polymetamorphic terrains: an example from the Proterozoic mobile belt of south India.
1088 *Contributions to Mineralogy and Petrology*, 131: 181-195.

1089 Be'eri-Shlevin, Y., Eyal, M., Eyal, Y., Whitehouse, M.J. and Litvinovsky, B., 2012. The Sa'al
1090 volcano-sedimentary complex (Sinai, Egypt): A latest Mesoproterozoic volcanic arc in
1091 the northern Arabian Nubian Shield. *Geology*, 40(5): 403-406.

1092 Be'eri-Shlevin, Y., Katzir, Y., Whitehouse, M.J. and Kleinhanns, I.C., 2009. Contribution of pre
1093 Pan-African crust to formation of the Arabian Nubian Shield: New secondary ionization
1094 mass spectrometry U-Pb and O studies of zircon. *Geology*, 37(10): 899-902.

1095 Berhe, S.M., 1981. The geology of the Dire Dawa area. *Memoir of the Ethiopian Institute of
1096 Geological Survey*.

1097 Bhaskar Rao, Y.J., Janardhan, A.S., Vijaya Kumar, T., Narayana, B.L., Dayal, A.M., Taylor,
1098 P.N. and Chetty, T.R.K., 2003. Sm-Nd model ages and Rb-Sr isotope systematics of
1099 charnockites and gneisses across the Cauvery Shear Zone, southern India: implications
1100 for the Archaean-Neoproterozoic boundary in the southern granulite terrain. In: M.
1101 Ranmakrishnan (Editor), *Tectonics of Southern Granulite Terrain*. Geological Society of
1102 India Memoir 50, pp. 297-317.

1103 Bingen, B., Jacobs, J., Viola, G., Henderson, I.H.C., Skar, O., Boyd, R., Thomas, R.J., Solli, A.,
1104 Key, R.M. and Daudi, E.X.F., 2009. Geochronology of the Precambrian crust in the
1105 Mozambique belt in NE Mozambique, and implications for Gondwana assembly.
1106 *Precambrian Research*, 170(3-4): 231-255.

1107 Bjerkgard, T., Stein, H.J., Bingen, B., Henderson, I.H.C., Sandstad, J.S. and Moniz, A., 2009.
1108 The Niassa Gold Belt, northern Mozambique - A segment of a continental-scale Pan-
1109 African gold-bearing structure? *Journal of African Earth Sciences*, 53(1-2): 45-58.

- 1110 Blades, M.L., Alessio, B.L., Collins, A.S., Foden, J., Payne, J.L., Glorie, S., Holden, P., Thorpe,
1111 B. and Al-Khirbash, S., 2020. Unravelling the Neoproterozoic accretionary history of
1112 Oman, using an array of isotopic systems in zircon. *Journal of the Geological Society*,
1113 177(2): 357-378.
- 1114 Blades, M.L., Collins Alan, S., Boone, S., Ekai, F., McIntyre, A. and Wilson, K., 2026.
1115 Unravelling the East African Orogen one terrane at a time: insights from NE Kenya,
1116 Australian Earth Science Convention, Melbourne, pp. 231.
- 1117 Blades, M.L., Collins, A.S., Foden, J., Payne, J.L., Stüwe, K., Abu-Alam, T., Makroum, F. and
1118 Hassan, M., 2021. Age and hafnium isotope evolution of Sudanese Butana and Chad
1119 illuminates the Stenian to Ediacaran evolution of the south and east Sahara. *Precambrian
1120 Research*, 362: 106323.
- 1121 Blades, M.L., Collins, A.S., Foden, J., Payne, J.L., Xu, X.C., Alemu, T., Woldetinsae, G., Clark,
1122 C. and Taylor, R.J.M., 2015. Age and hafnium isotopic evolution of the Didesa and
1123 Kemashi Domains, western Ethiopia. *Precambrian Research*, 270: 267-284.
- 1124 Blades, M.L., Foden, J., Collins, A.S., Alemu, T. and Woldetinsae, G., 2019. The origin of the
1125 ultramafic rocks of the Tulu Dimtu Belt, western Ethiopia - do they represent remnants of
1126 the Mozambique Ocean? *Geological Magazine*, 156(1): 62-82.
- 1127 Boger, S.D., Hirdes, W., Ferreira, C.A.M., Jenett, T., Dallwig, R. and Fanning, C.M., 2015. The
1128 580-520 Ma Gondwana suture of Madagascar and its continuation into Antarctica and
1129 Africa. *Gondwana Research*, 28(3): 1048-1060.
- 1130 Boger, S.D., Hirdes, W., Ferreira, C.A.M., Schulte, B., Jenett, T. and Fanning, C.M., 2014. From
1131 passive margin to volcano-sedimentary forearc: The Tonian to Cryogenian evolution of
1132 the Anosyen Domain of southeastern Madagascar. *Precambrian Research*, 247: 159-186.
- 1133 Boger, S.D., Maas, R., Pastuhov, M., Macey, P.H., Hirdes, W., Schulte, B., Fanning, C.M.,
1134 Ferreira, C.A.M., Jenett, T. and Dallwig, R., 2019. The tectonic domains of southern and
1135 western Madagascar. *Precambrian Research*, 327: 144-175.
- 1136 Bowden, S., Gani, N.D., Alemu, T., O'Sullivan, P., Abebe, B. and Tadesse, K., 2020. Evolution
1137 of the Western Ethiopian Shield revealed through U-Pb geochronology, petrogenesis, and
1138 geochemistry of syn- and post-tectonic intrusive rocks. *Precambrian Research*, 338.
- 1139 Brandt, S., Schenk, V., Raith, M.M., P., A., Gerdes, A. and Srikantappa, C., 2011. Late
1140 Neoproterozoic P-T evolution of HP-UHT granulites from the Palni Hills (South India):
1141 New constraints from phase diagram modelling, LA-ICP-MS zircon dating and in-situ
1142 EMP monazite dating. *Journal of Petrology*, 52: 1813-1856.
- 1143 Brown, M. and Johnson, T., 2019. Metamorphism and the evolution of subduction on Earth.
1144 *American Mineralogist*, 104(8): 1065-1082.
- 1145 Burke, K., Dewey, J.F. and Kidd, W.S.F., 1976. Precambrian Paleomagnetic Results Compatible
1146 with Contemporary Operation of Wilson Cycle. *Tectonophysics*, 33(3-4): 287-299.
- 1147 Candan, O., Koraly, O.E., Topuz, G., Oberhansli, R., Fritz, H., Collins, A.S. and Chen, F.,
1148 2016. Late Neoproterozoic gabbro emplacement followed by early Cambrian eclogite-
1149 facies metamorphism in the Menderes Massif (W. Turkey): Implications on the final
1150 assembly of Gondwana. *Gondwana Research*, 34: 158-173.
- 1151 Cao, X.Z., Collins, A.S., Pisarevsky, S., Flament, N., Li, S.Z., Hasterok, D. and Müller, R.D.,
1152 2024. Earth's tectonic and plate boundary evolution over 1.8 billion years. *Geoscience
1153 Frontiers*, 15(6).

1154 Cawood, P.A., 2005. Terra Australis Orogen: Rodinia breakup and development of the Pacific
1155 and Iapetus margins of Gondwana during the Neoproterozoic and Paleozoic. *Earth*
1156 *Science Reviews.*, 69: 249-279.

1157 Cawood, P.A. and Buchan, C., 2007. Linking accretionary orogenesis with supercontinent
1158 assembly. *Earth Science Reviews.*, 82: 217-256.

1159 Cawood, P.A., Zhao, G.C., Yao, J.L., Wang, W., Xu, Y.J. and Wang, Y.J., 2018. Reconstructing
1160 South China in Phanerozoic and Precambrian supercontinents. *Earth-Science Reviews*,
1161 186: 173-194.

1162 Cenko, B., Braun, I. and Bröcker, M., 2004. Evolution of the continental crust in the Kerala
1163 Khondalite Belt, southernmost India: evidence from Nd isotope mapping, U–Pb and Rb–
1164 Sr geochronology. *Precambrian Research*, 134: 275-292.

1165 Chen, X., Zhou, Y. and Shields, G.A., 2022. Progress towards an improved Precambrian
1166 seawater $^{87}\text{Sr}/^{86}\text{Sr}$ curve. *Earth-Science Reviews*, 224: 103869.

1167 Clark, C., Collins, A.S., Santosh, M., Taylor, R. and Wade, B.P., 2009. The P-T-t architecture of
1168 a Gondwanan suture: REE, U-Pb and Ti-in-zircon thermometric constraints from the
1169 Palghat Cauvery shear system, South India. *Precambrian Research*, 174(1-2): 129-144.

1170 Clark, C., Collins, A.S., Taylor, R.J.M. and Hand, M., 2020. Isotopic systematics of zircon
1171 indicate an African affinity for the rocks of southernmost India. *Scientific Reports*.

1172 Clark, C., Healy, D., Johnson, T., Collins, A.S., Taylor, R.J., Santosh, M. and Timms, N.E.,
1173 2015. Hot orogens and supercontinent amalgamation: A Gondwanan example from
1174 southern India. *Gondwana Research*, 28(4): 1310-1328.

1175 Cohen, K., Harper, D., Gibbard, P. and Car, N., 2025. The ICS international chronostratigraphic
1176 chart this decade. *Episodes* 48.

1177 Collins, A., 2006. The tectonic evolution of Madagascar: Its place in the East African orogen.
1178 *Gondwana Research*, 3(4): 549-552.

1179 Collins, A. and Pisarevsky, S., 2005. Amalgamating eastern Gondwana: The evolution of the
1180 Circum-Indian Orogens. *Earth-Science Reviews*, 71(3-4): 229-270.

1181 Collins, A. and Windley, B., 2002. The tectonic evolution of central and northern Madagascar
1182 and its place in the final assembly of Gondwana. *Journal of Geology*, 110(3): 325-339.

1183 Collins, A.S., Ali, J.R. and Razakamanana, T., 2022a. An Introduction to the Geology of
1184 Madagascar. In: S.M. Goodman (Editor), *The new natural history of Madagascar*.
1185 Princeton University Press, Princeton, pp. 45-51.

1186 Collins, A.S., Blades, M.L. and Merdith, A.S., 2021a. The Arabian–Nubian Shield Within the
1187 Neoproterozoic Plate Tectonic Circuit. In: Z. Hamimi, A.-R. Fowler, J.-P. Liégeois, A.
1188 Collins, M.G. Abdelsalam and M. Abd Ei-Wahed (Editors), *The Geology of the Arabian-*
1189 *Nubian Shield*. Springer International Publishing, Cham, pp. 195-202.

1190 Collins, A.S., Blades, M.L., Merdith, A.S. and Foden, J.D., 2021b. Closure of the Proterozoic
1191 Mozambique Ocean was instigated by a late Tonian plate reorganization event.
1192 *Communications Earth & Environment*, 2(1).

1193 Collins, A.S., Cameron, F., Blades, M.L., Hasterok, D., Simpson, A., Gilbert, S., Clark, C. and
1194 Makin, S., 2022b. Size is everything: reconstructing the East African Orogen—a
1195 Gondwanan supermountain—as a critical step to modelling the Neoproterozoic earth
1196 system, Goldschmidt, Hawaii.

1197 Collins, A.S., Clark, C. and Plavsa, D., 2014. Peninsular India in Gondwana: The tectonothermal
1198 evolution of the Southern Granulite Terrain and its Gondwanan counterparts. *Gondwana*
1199 *Research*, 25(1): 190-203.

- 1200 Collins, A.S., Clark, C., Sajeev, K., Santosh, M., Kelsey, D.E. and Hand, M., 2007. Passage
1201 through India: the Mozambique Ocean suture, high-pressure granulites and the Palghat-
1202 Cauvery shear zone system. *Terra Nova*, 19(2): 141-147.
- 1203 Collins, A.S., Kinny, P.D. and Razakamanana, T., 2012. Depositional age, provenance and
1204 metamorphic age of metasedimentary rocks from southern Madagascar. *Gondwana
1205 Research*, 21(2-3): 353-361.
- 1206 Collins, A.S., Kröner, A., Fitzsimons, I.C.W. and Razakamanana, T., 2003. Detrital Footprint of
1207 the Mozambique Ocean: U/Pb SHRIMP and Pb Evaporation Zircon Geochronology of
1208 Metasedimentary Gneisses in Eastern Madagascar. *Tectonophysics*, 375: 77-99.
- 1209 Collins, A.S., Redaa, A., Vecoli, M. and Alwaheed, A., 2024. Age of the basement to the
1210 Arabian petroleum system: U-Pb zircon/apatite and in-situ Rb-Sr LA-ICP-MS/MS dates
1211 from beneath central and east Saudi Arabia, AAPG ICE 2024, Muscat.
- 1212 Coolen, J.J.M.M., Priem, H.N.A., Verdurmen, E.A.T. and Verschure, R.H., 1982. Possible
1213 zircon U-Pb evidence for Pan-African granulite-facies metamorphism in the Mozambique
1214 belt of southern Tanzania. *Precambrian Research*, 17: 31-40.
- 1215 Costa, R.L., Schmitt, R.S., Collins, A.S., Armistead, S.E., Gomes, I.V., Archibald, D.B. and
1216 Razakamanana, T., 2021. Tectonic evolution of an Early Cryogenian late-magmatic basin
1217 in central Madagascar. *Journal of African Earth Sciences*, 179: 104205.
- 1218 Cox, G.M., Foden, J. and Collins, A.S., 2019. Late Neoproterozoic adakitic magmatism of the
1219 eastern Arabian Nubian Shield. *Geoscience Frontiers*, 10(6): 1981-1992.
- 1220 Cox, G.M., Halverson, G.P., Stevenson, R.K., Vokaty, M., Poirier, A., Kunzmann, M., Li, Z.X.,
1221 Denyszyn, S.W., Strauss, J.V. and Macdonald, F.A., 2016a. Continental flood basalt
1222 weathering as a trigger for Neoproterozoic Snowball Earth. *Earth and Planetary Science
1223 Letters*, 446: 89-99.
- 1224 Cox, G.M., Jarrett, A., Edwards, D., Crockford, P.W., Halverson, G.P., Collins, A.S., Poirier, A.
1225 and Li, Z.X., 2016b. Basin redox and primary productivity within the Mesoproterozoic
1226 Roper Seaway. *Chemical Geology*, 440: 101-114.
- 1227 Cox, G.M., Lewis, C.J., Collins, A.S., Halverson, G.P., Jourdan, F., Foden, J., Nettle, D. and
1228 Kattan, F., 2012. Ediacaran terrane accretion within the Arabian-Nubian Shield.
1229 *Gondwana Research*, 21(2-3): 341-352.
- 1230 Cox, R., Armstrong, R.A. and Ashwal, L.D., 1998. Sedimentology, geochronology and
1231 provenance of the Proterozoic Itremo Group, central Madagascar, and implications for
1232 pre-Gondwana palaeogeography. *Journal of the Geological Society, London*, 155: 1009-
1233 1024.
- 1234 Cox, R., Coleman, D., Chokel, C., DeOreo, S., Wooden, J., Collins, A., De Waele, B. and
1235 Kroner, A., 2004. Proterozoic tectonostratigraphy and paleogeography of central
1236 Madagascar derived from detrital zircon U-Pb age populations. *Journal of Geology*,
1237 112(4): 379-399.
- 1238 Cozzi, A., Rea, G. and Craig, J., 2012. From global geology to hydrocarbon exploration:
1239 Ediacaran-Early Cambrian petroleum plays of India, Pakistan and Oman. *Geological
1240 Society, London, Special Publications*, 366(1): 131-162.
- 1241 Cutten, H., Johnson, S.P. and De Waele, B., 2006. Protolith Ages and Timing of Metasomatism
1242 Related to the Formation of Whiteschists at Mautia Hill, Tanzania: Implications for the
1243 Assembly of Gondwana. *Journal of Geology*, 114: 683-698.
- 1244 Dal Piaz, G.V., Ibrahim, H.A., Martin, S., Piccardo, G.B., Rigatti, G. and Venturelli, G., 1993.
1245 Pan-African Metabasalts from the Maydh Area, North-Eastern Somalia. In: E. Abbate,

1246 M. Sagri and F.P. Sassi (Editors), *Geology and Mineral Resources of Somalia and*
1247 *Surrounding Regions*. Instituto Agronomico per l'Oltremare, Firenze, pp. 41-58.

1248 Dalziel, I.W.D., 1997. Neoproterozoic-Paleozoic geography and tectonics: Review, hypothesis,
1249 environmental speculation. *Geological Society of America Bulletin*, 109(1): 16-42.

1250 Davies, R.G. and Crawford, A.R., 1971. Petrography and Age of Rocks of Bulland-Hill, Kirana-
1251 Hills, Sarghoda District, West Pakistan. *Geological Magazine*, 108(3): 235-&.

1252 de Wall, H., Regelous, A., Tomaschek, F., Bestmann, M., Hahn, G. and Sharma, K.K., 2022.
1253 Tonian evolution of an active continental margin - a model for Neoproterozoic NW
1254 India-SE Pakistan-E Oman linkage. *Precambrian Research*, 381: 106822.

1255 de Wit, M.J. and Linol, B., 2015. Precambrian Basement of the Congo Basin and Its Flanking
1256 Terrains. In: M.J. de Wit, F. Guillocheau and M.C.J. de Wit (Editors), *Geology and*
1257 *Resource Potential of the Congo Basin*. Regional Geology Reviews. Springer-Verlag,
1258 Berlin Heidelberg, pp. 19--37.

1259 Deb, M., Thorpe, R.I., Krstic, D., Corfu, F. and Davis, D.W., 2001. Zircon U-Pb and galena Pb
1260 isotope evidence for an approximate 1.0 Ga terrane constituting the western margin of the
1261 Aravalli-Delhi orogenic belt, northwestern India. *Precambrian Research*, 108: 195-213.

1262 Derry, L.A. and France-Lanord, C., 1996. Neogene Himalayan weathering history and
1263 river ⁸⁷Sr/⁸⁶Sr: impact on the marine Sr record. *Earth and Planetary Science Letters*,
1264 142(1): 59-74.

1265 Djerosse, F., Berger, J., Vanderhaeghe, O., Isseini, M., Ganne, J. and Zeh, A., 2020.
1266 Neoproterozoic magmatic evolution of the southern Ouaddaï Massif (Chad) Open
1267 Access. *Bulletin de la Societe Geologique de France*, 191: 34.

1268 Doebrich, J.L., Al-Jehani, A.M., Siddiqui, A.A., Hayes, T.S., Wooden, J.L. and Johnson, P.R.,
1269 2007. Geology and metalogeny of the Ar Rayn terrane, eastern Arabian shield: Evolution
1270 of a Neoproterozoic continental-margin arc during assembly of Gondwana within the
1271 East African orogen. *Precambrian Research*, 158: 17-50.

1272 Domeier, M., 2016. A plate tectonic scenario for the Iapetus and Rheic oceans. *Gondwana*
1273 *Research*, 36: 275-295.

1274 Domeier, M. and Torsvik, T.H., 2014. Plate tectonics in the late Paleozoic. *Geoscience Frontiers*,
1275 5(3): 303-350.

1276 Drury, S.A. and De Souza, C.R., 1998. Neoproterozoic terrane assemblages in Eritrea: review
1277 and prospects. *Journal of African Earth Sciences*, 27(3-4): 331-348.

1278 Eguíluz, L., Puellas, P., Tarrío, A. and Abalos, B., 2024. The Neoproterozoic Mozambique Belt
1279 in the Gol Mountains (N Tanzania): Structural Analysis of Amphibolite and Granulite-
1280 Facies Nappe Tectonites From a Crustal Orogenic Channel. *Tectonics*, 43(11).

1281 Elburg, M.A., Andersen, T., Jacobs, J., Laufer, A., Ruppel, A., Krohne, N. and Damaske, D.,
1282 2016. One Hundred Fifty Million Years of Intrusive Activity in the Sor Rondane
1283 Mountains (East Antarctica): Implications for Gondwana Assembly. *Journal of Geology*,
1284 124(1): 1-26.

1285 Eyal, M., Be'eri-Shlevin, Y., Eyal, Y., Whitehouse, M.J. and Litvinovsky, B., 2014. Three
1286 successive Proterozoic island arcs in the Northern Arabian-Nubian Shield: Evidence from
1287 SIMS U-Pb dating of zircon. *Gondwana Research*, 25(1): 338-357.

1288 Fergusson, C.L., Nutman, A.P., Mohajjel, M. and Bennett, V.C., 2016. The Sanandaj-Sirjan
1289 Zone in the Neo-Tethyan suture, western Iran: Zircon U-Pb evidence of late Palaeozoic
1290 rifting of northern Gondwana and mid-Jurassic orogenesis. *Gondwana Research*, 40: 43-
1291 57.

1292 Flowerdew, M.J., Whitehouse, M.J. and Stoesser, D.B., 2013. The Nabitah fault zone, Saudi
1293 Arabia: A Pan-African suture separating juvenile oceanic arcs. *Precambrian Research*,
1294 239: 95-105.

1295 Frisch, W. and Pohl, W., 1986. Petrochemistry of some mafic and ultramafic rocks from the
1296 Mozambique Belt, SE Kenya. *Mitteilungen der Oesterreichischen Geologischen*
1297 *Gesellschaft*, 78: 97-114.

1298 Fritz, H., Abdelsalam, M., Ali, K.A., Bingen, B., Collins, A.S., Fowler, A.R., Ghebreab, W.,
1299 Hauzenberger, C.A., Johnson, P., Kusky, T., Macey, P., Muhongo, S., Stern, R.J. and
1300 Viola, G., 2013. Orogen styles in the East Africa Orogens: A review of the
1301 Neoproterozoic to Cambrian Tectonic Evolution. *Journal of African Earth Sciences*, 86:
1302 65-106.

1303 Fritz, H. and Hauzenberger, C., 2021. The Southern Part of the Arabian–Nubian Shield in Kenya
1304 and Tanzania. In: Z. Hamimi, A.-R. Fowler, J.-P. Liégeois, A. Collins, M.G. Abdelsalam
1305 and M. Abd Ei-Wahed (Editors), *The Geology of the Arabian-Nubian Shield*. Springer
1306 International Publishing, Cham, pp. 63-80.

1307 Gessner, K., Collins, A., Ring, U. and Gungor, T., 2004. Structural and thermal history of poly-
1308 orogenic basement: U-Pb geochronology of granitoid rocks in the southern Menderes
1309 Massif, Western Turkey. *Journal of the Geological Society*, 161: 93-101.

1310 Ghosh, J.G., de Wit, M.J. and Zartman, R.E., 2004. Age and tectonic evolution of
1311 Neoproterozoic ductile shear zones in the Southern Granulite Terrain of India, with
1312 implications for Gondwana studies. *Tectonics*, 23(TC3006): doi:10.1029/2002TC001444.

1313 Glen, R.A. and Meffre, S., 2009. Styles of Cenozoic collisions in the western and southwestern
1314 Pacific and their applications to Palaeozoic collisions in the Tasmanides of eastern
1315 Australia. *Tectonophysics*, 479(1-2): 130-149.

1316 Godderis, Y., Donnadieu, Y., Carretier, S., Aretz, M., Dera, G., Macouin, M. and Regard, V.,
1317 2017. Onset and ending of the late Palaeozoic ice age triggered by tectonically paced
1318 rock weathering. *Nature Geoscience*, 10(5): 382-+.

1319 Gomes, I.V., Schmitt, R.S., Rosenbaum, G., Armistead, S.E. and Mussili, J.V.S., 2025. The
1320 triple orogenic junction of central Gondwana. *International Geology Review*, 67(12):
1321 1533-1560.

1322 Gómez-Pérez, I. and Morton, A., 2025. Neoproterozoic–early Paleozoic tectonic evolution of
1323 Oman revisited: implications for the consolidation of Gondwana. *Geological Society*,
1324 London, Special Publications, 550(1): SP550-2024-36.

1325 Gómez-Pérez, I., Morton, A., Rawahi, H.A. and Frei, D., 2024. Oman as a fragment of Ediacaran
1326 eastern Gondwana. *Geology*, 52(6): 473-478.

1327 Goscombe, B., Foster, D.A., Gray, D. and Wade, B., 2020. Assembly of central Gondwana along
1328 the Zambezi Belt: Metamorphic response and basement reactivation during the Kuunga
1329 Orogeny. *Gondwana Research*, 80: 410-465.

1330 Goscombe, B., Foster, D.A., Gray, D., Wade, B., Marsellos, A. and Titus, J., 2017. Deformation
1331 correlations, stress field switches and evolution of an orogenic intersection: The Pan-
1332 African Kaoko-Damara orogenic junction, Namibia. *Geoscience Frontiers*, 8(6): 1187-
1333 1232.

1334 Gregory, L.C., Meert, J.G., Bingen, B., Pandit, M.K. and Torsvik, T.H., 2009. Paleomagnetism
1335 and geochronology of the Malani Igneous Suite, Northwest India: Implications for the
1336 configuration of Rodinia and the assembly of Gondwana. *Precambrian Research*, 170(1-
1337 2): 13-26.

1338 Guru Rajesh, K. and Chetty, T.R.K., 2006. Structure and tectonics of the Achancovil Shear
1339 Zone, southern India. *Gondwana Research*, 10: 86-98.

1340 Halverson, G.P., Hurtgen, M., Porter, S.M. and Collins, A.S., 2010. Neoproterozoic-Cambrian
1341 Biogeochemical Evolution. In: C. Gaucher, A. Sial, G.P. Halverson and H. Frimmel
1342 (Editors), *Events at the Precambrian-Cambrian boundary: a focus on southwestern*
1343 *Gondwana*. Elsevier, *Developments in Precambrian Geology*, Amsterdam.

1344 Hamimi, Z., Eldosouky, A.M., Hagag, W. and Kamh, S.Z., 2023. Large-scale geological
1345 structures of the Egyptian Nubian Shield. *Scientific Reports*, 13(1): 1923.

1346 Handke, M.J., Tucker, R.D. and Hamilton, M.A., 1997. Early Neoproterozoic (800-790 Ma)
1347 intrusive igneous rocks in central Madagascar; geochemistry and petrogenesis. *Abstracts*
1348 *with Programs*, 29: 468.

1349 Harms, U., Darbyshire, D.P.F., Denkler, T., Hengst, M. and Schandelmeier, H., 1994. Evolution
1350 of the Neoproterozoic Delgo Suture Zone and crustal growth in northern Sudan:
1351 geochemical and radiogenic isotope constrains. *Geologische Rundschau*, 83: 591–603.

1352 Hasterok, D. and Chapman, D.S., 2007. Continental thermal isostasy: 1. Methods and sensitivity.
1353 *Journal of Geophysical Research: Solid Earth*, 112(B6).

1354 Hauzenberger, C.A., Sommer, H., Fritz, H., Bauernhofer, A., Kröner, A., Hoinkes, G.,
1355 Wallbrecher, E. and Thöni, M., 2007. SHRIMP U-Pb zircon and Sm-Nd garnet ages from
1356 the granulite facies basement of SE-Kenya: evidence for Neoproterozoic polycyclic
1357 assembly of the Mozambique Belt. *Journal of the Geological Society, London*, 164: 189-
1358 201.

1359 Honarmand, M., Xiao, W.J., Nabatian, G., Blades, M.L., dos Santos, M.C., Collins, A.S. and Ao,
1360 S.J., 2018. Zircon U-Pb-Hf isotopes, bulk-rock geochemistry and Sr-Nd-Pb isotopes from
1361 late Neoproterozoic basement in the Mahneshan area, NW Iran: Implications for
1362 Ediacaran active continental margin along the northern Gondwana and constraints on the
1363 late Oligocene crustal anatexis. *Gondwana Research*, 57: 48-76.

1364 Jacobs, J., Elburg, M., Laufer, A., Kleinhanns, I.C., Henjes-Kunst, F., Estrada, S., Ruppel, A.S.,
1365 Damaske, D., Montero, P. and Bea, F., 2015. Two distinct Late Mesoproterozoic/Early
1366 Neoproterozoic basement provinces in central/eastern Dronning Maud Land, East
1367 Antarctica: The missing link, 15-21 degrees E. *Precambrian Research*, 265: 249-272.

1368 Jamshidi-Badr, M., Collins, A.S., Masoudi, F., Cox, G. and Mohajel, M., 2013. The U-Pb age,
1369 geochemistry and tectonic significance of granitoids in The Soursat complex, Northwest
1370 Iran. *Turkish Journal of Earth Sciences*, 22: 1-31.

1371 John, T., Schenk, V., Mezger, K. and Tembo, F., 2004. Timing and PT evolution of whiteschist
1372 metamorphism in the Lufilian Arc-Zambezi Belt Orogen (Zambia): Implications for the
1373 assembly of Gondwana. *Journal of Geology*, 112(1): 71-90.

1374 Johnson, P.R., Andresen, A., Collins, A.S., Fowler, A.R., Fritz, H., Ghebreab, W., Kusky, T. and
1375 Stern, R.J., 2011. Late Cryogenian-Ediacaran history of the Arabian-Nubian Shield: A
1376 review of depositional, plutonic, structural, and tectonic events in the closing stages of
1377 the northern East African Orogen. *Journal of African Earth Sciences*, 61(3): 167-232.

1378 Johnson, P.R. and Stewart, I.C.F., 1995. Magnetically inferred basement structure in central
1379 Saudi Arabia. *Tectonophysics*, 245: 37-52.

1380 Johnson, P.R. and Woldehaimanot, B., 2003. Development of the Arabian-Nubian Shield:
1381 perspectives on accretion and deformation in the northern East African Orogen and the
1382 assembly of Gondwana. In: M. Yoshida, B.F. Windley and S. Dasgupta (Editors),

1383 Proterozoic East Gondwana: Supercontinent Assembly and Breakup. Geological Society,
1384 London, Special Publication 206, pp. 289-325.

1385 Johnson, S.P., Cutten, H.N.C., Muhongo, S. and De Waele, B., 2003. Neoproterozoic magmatism
1386 and metamorphism of the western granulites in the central domain of the Mozambique
1387 belt, Tanzania: U-Pb SHRIMP geochronology and PT estimates. *Tectonophysics*, 375:
1388 125-145.

1389 Johnson, S.P., De Waele, B. and Liyungu, K.A., 2006. U-Pb sensitive high-resolution ion
1390 microprobe (SHRIMP) zircon geochronology of granitoid rocks in eastern Zambia:
1391 Terrane subdivision of the Mesoproterozoic Southern Irumide Belt - art. no. TC6004.
1392 *Tectonics*, 25(6): C6004-C6004.

1393 Johnson, T.E., Clark, C., Taylor, R.J.M., Santosh, M. and Collins, A.S., 2015. Prograde and
1394 retrograde growth of monazite in migmatites: An example from the Nagercoil Block,
1395 southern India. *Geoscience Frontiers*, 6(3): 373-387.

1396 Jöns, N. and Schenk, V., 2008. Relics of the Mozambique Ocean in the central East African
1397 Orogen: evidence from the Vohibory Block of southern Madagascar. *Journal of*
1398 *Metamorphic Geology*, 26: 17-28.

1399 Jöns, N., Schenk, V., John, T. and Razakamanana, T., 2005. Relics of the Mozambique Ocean:
1400 geochemistry of the Vohibory Block (Madagascar). In: M.T.D. Wingate and S.A.
1401 Pisarevsky (Editors), *Supercontinents and Earth Evolution*. Geological Society of
1402 Australia, Abstracts, No. 81, Fremantle, pp. 133.

1403 Just, J., Schulz, B., de Wall, H., Jourdan, F. and Pandit, M.K., 2011. Monazite CHIME/EPMA
1404 dating of Erinpura granitoid deformation: Implications for Neoproterozoic tectono-
1405 thermal evolution of NW India. *Gondwana Research*, 19(2): 402-412.

1406 Kashghari, W., Collins, A.S., Nehlig, P., Abu El-Enen, M.M., Macey, P.H., Jacobs, J., Passchier,
1407 C., Kattan, F.H., Whitehouse, M., Bakhsh, R., Al Garni, S.M., Elkomi, M.B., Johnson,
1408 P.R., Stern, R.J., Harbi, F.M.H., Rimi, N.N. and Qubsani, A.N., 2025. Critical Review of
1409 the Stratigraphy Framework of the Arabian Shield: Current Understanding and
1410 Knowledge Gaps. Saudi Geological Survey Special Publication Report.

1411 Kazmin, V., 1975. Explanation of the geological map of Ethiopia. Memoir of the Ethiopian
1412 Institute of Geological Survey.

1413 Kitano, I., Osanai, Y., Nakano, N., Adachi, T. and Fitzsimons, I.C.W., 2018. Detrital zircon and
1414 igneous protolith ages of high-grade metamorphic rocks in the Highland and Wann
1415 Complexes, Sri Lanka: Their geochronological correlation with southern India and East
1416 Antarctica. *Journal of Asian Earth Sciences*, 156: 122-144.

1417 Koralay, O.E., Dora, O.O., Chen, F., Satir, M. and Candan, O., 2004. Geochemistry and
1418 geochronology of orthogneisses in the derbent (Alasehir) area, eastern part of the
1419 Odemis-Kiraz submassif, Menderes Massif: Pan-African magmatic activity. *Turkish*
1420 *Journal of Earth Sciences*, 13(1): 37-61.

1421 Kröner, A., Hegner, E., Collins, A., Windley, B., Brewer, T., Razakamanana, T. and Pidgeon, R.,
1422 2000. Age and magmatic history of the Antananarivo Block, central Madagascar, as
1423 derived from zircon geochronology and Nd isotopic systematics. *American Journal of*
1424 *Science*, 300(4): 251-288.

1425 Kröner, A. and Jaekel, P., 1994. Zircon ages from rocks of the Wann complex, Sri Lanka.
1426 *Journal of the Geological Society of Sri Lanka*, 5: 41-57.

1427 Kröner, A., Kovach, V., Belousova, E., Hegner, E., Armstrong, R., Dolgoplova, A., Seltmann,
1428 R., Alexeiev, D.V., Hoffmann, J.E., Wong, J., Sun, M., Cai, K., Wang, T., Tong, Y.,

1429 Wilde, S.A., Degtyarev, K.E. and Rytisk, E., 2014. Reassessment of continental growth
1430 during the accretionary history of the Central Asian Orogenic Belt. *Gondwana Research*,
1431 25(1): 103-125.

1432 Kröner, A., Muhongo, S., Hegner, E. and Wingate, M.T.D., 2003. Single-zircon geochronology
1433 and Nd isotopic systematics of Proterozoic high-grade rocks from the Mozambique belt
1434 of southern Tanzania (Masasi area): implications for Gondwana assembly. *Journal of the*
1435 *Geological Society, London*, 160: 745-757.

1436 Kroner, A., Sacchi, R., Jaeckel, P. and Costa, M., 1997. Kibaran magmatism and Pan-African
1437 granulite metamorphism in northern Mozambique: single zircon ages and regional
1438 implications. *Journal of African Earth Sciences*, 25(3): 467-484.

1439 Kröner, A., Santosh, M. and Wong, J., 2012. Zircon ages and Hf isotopic systematics reveal
1440 vestiges of Mesoproterozoic to Archaean crust within the late Neoproterozoic–Cambrian
1441 high-grade terrain of southernmost India. *Gondwana Research*, 21: 876-886.

1442 Kröner, A. and Sassi, F.P., 1996. Evolution of the northern Somali basement: new constraints
1443 from zircon ages. *Journal of African Earth Sciences*, 22: 1-15.

1444 Kumar, T.V., Rao, Y.J.B., Plavsa, D., Collins, A.S., Tomson, J.K., Gopal, B.V. and Babu,
1445 E.V.S.S.K., 2017. Zircon U-Pb ages and Hf isotopic systematics of charnockite gneisses
1446 from the Ediacaran-Cambrian high-grade metamorphic terranes, southern India:
1447 Constraints on crust formation, recycling, and Gondwana correlations. *Geological*
1448 *Society of America Bulletin*, 129(5-6): 625-648.

1449 Kusky, T.M. and Matsah, M.I., 2003. Neoproterozoic dextral faulting on the Najd Fault System,
1450 Saudi Arabia, preceded sinistral faulting and escape tectonics related to closure of the
1451 Mozambique Ocean. In: M. Yoshida, B. Windley and S. Dasgupta (Editors), *Proterozoic*
1452 *East Gondwana: Supercontinent Assembly and Breakup*. Geological Society, London,
1453 Special Publication 206, pp. 327-361.

1454 Küster, D., Utke, A., Leupolt, L., Lenoir, J.L. and Haider, A., 1990. Pan-African granitoid
1455 magmatism in northeastern and southern Somalia. *Berliner Geowissenschaftliche*
1456 *Abhandlungen*, 120: 519-536.

1457 Lenoir, J.-L., Küster, D., Liégeois, J.-P., Utke, A., Haider, A. and Matheis, G., 1994. Origin and
1458 regional significance of late Precambrian and early Palaeozoic granitoids in the Pan-
1459 African belt of Somalia. *Geologische Rundschau*, 83: 624-641.

1460 Li, Z.-X., Liu, Y. and Ernst, R., 2023. A dynamic 2000—540 Ma Earth history: From cratonic
1461 amalgamation to the age of supercontinent cycle. *Earth-Science Reviews*, 238: 104336.

1462 Li, Z.X., Bogdanova, S.V., Collins, A.S., Davidson, A., De Waele, B., Ernst, R.E., Fitzsimons,
1463 I.C.W., Fuck, R.A., Gladkochub, D.P., Jacobs, J., Karlstrom, K.E., Lu, S., Natapov, L.M.,
1464 Pease, V., Pisarevsky, S.A., Thrane, K. and Vernikovsky, V., 2008. Assembly,
1465 configuration, and break-up history of Rodinia: A synthesis. *Precambrian Research*,
1466 160(1-2): 179-210.

1467 Lom, N., Şengör, A.M.C., Zabcı, C., Sunal, G. and Öner, T., 2024. The Saharides: Reassessing
1468 the Nature and History of the Pan-African Events in North Africa and the Arabian Shield.
1469 In: Z. Hamimi, M.C. Chabou, E. Errami, A.-R. Fowler, N. Fello, A. Masrouhi and R.
1470 Leprêtre (Editors), *The Geology of North Africa*. Regional Geology Reviews. Springer.

1471 Loosveld, R., Bell, A. and Terken, J., 1996. The tectonic evolution of Interior Oman. *Georabia*,
1472 1: 28-51.

- 1473 Maboko, M.A.H., 2000. Nd and Sr isotopic investigation of the Archean–Proterozoic boundary
1474 in north eastern Tanzania: constraints on the nature of Neoproterozoic tectonism in the
1475 Mozambique Belt. *Precambrian Research*, 102(1): 87-98.
- 1476 Mänttari, I., Kigireigu, F., Huhma, H., Kock, G.S., Koistinen, T., Kuosmanen, E.T., Lahaye, Y.,
1477 Lehtonen, M.I., Mäkitie, H., Manninen, T., O'Brien, H., Saalman, K., Virransalo, P. and
1478 Westerhof, A., 2011. New Precambrian rock ages from Uganda. Abstracts Volume, 23rd
1479 Colloquium of African Geology, 8-14 January 2011, Johannesburg, South Africa.
- 1480 McIntyre, A., 2023. High-grade metamorphism in Turkana, Kenya: implications for the
1481 evolution of the East African Orogen, The University of Adelaide, Adelaide, 94 pp.
- 1482 McWilliams, M.O., 1981. Palaeomagnetism and Precambrian tectonic evolution of Gondwana.
1483 In: A. Kröner (Editor), *Precambrian Plate Tectonics*. Elsevier, Amsterdam, pp. 649-687.
- 1484 Meert, J.G., Pandit, M.K. and Kamenov, G.D., 2013. Further geochronological and
1485 paleomagnetic constraints on Malani (and pre-Malani) magmatism in NW India.
1486 *Tectonophysics*, 608: 1254-1267.
- 1487 Meert, J.G. and Van der Voo, R., 1997. The assembly of Gondwana 800-550 Ma. *Journal of*
1488 *Geodynamics*, 23: 223-236.
- 1489 Merdith, A.S., Collins, A.S., Williams, S.E., Pisarevsky, S., Foden, J.D., Archibald, D.B.,
1490 Blades, M.L., Alessio, B.L., Armistead, S., Plavsa, D., Clark, C. and Muller, R.D., 2017a.
1491 A full-plate global reconstruction of the Neoproterozoic. *Gondwana Research*, 50: 84-
1492 134.
- 1493 Merdith, A.S., Williams, S.E., Collins, A.S., Tetley, M.G., Mulder, J.A., Blades, M.L., Young,
1494 A., Armistead, S.E., Cannon, J., Zahirovic, S. and Müller, R.D., 2021. Extending full-
1495 plate tectonic models into deep time: Linking the Neoproterozoic and the Phanerozoic.
1496 *Earth-Science Reviews*, 214: 103477.
- 1497 Merdith, A.S., Williams, S.E., Muller, R.D. and Collins, A.S., 2017b. Kinematic constraints on
1498 the Rodinia to Gondwana transition. *Precambrian Research*, 299: 132-150.
- 1499 Merdith, A.S., Wright, N.M., Williams, S., Hunter, S.J., J., L., Blades, M.L., F., B., Supadee, K.,
1500 Gurung, K., Xu, Z., Hasterok, D., Collins, A.S. and Mills, B.J.W., Submitted. Process-
1501 based simulation of palaeogeography and topography over the 1 last billion years. *Earth-*
1502 *Science Reviews*.
- 1503 Meyer, S.E., Passchier, C., Abu-Alam, T. and Stüwe, K., 2014. A strike-slip core complex from
1504 the Najd fault system, Arabian shield. *Terra Nova*, 26(5): 387-394.
- 1505 Mills, B.J.W., le Hir, G., Merdith, A., Gurung, K., Bowyer, F.T., Krause, A.J., Sanchez-
1506 Baracaldo, P., Hunter, S.J. and Zhang, Y., 2025. Exploring Neoproterozoic climate and
1507 biogeochemical evolution in the SCION model. *Global and Planetary Change*, 249:
1508 104791.
- 1509 Mohammed, M.A.I., 2017. The geology of the western Nuba Mountains region, South Kordofan
1510 State, Sudan, with special emphasis on the low-grade Neoproterozoic meta-volcano-
1511 sedimentary sequence, University of Pretoria, 200 pp.
- 1512 Mole, D.R., Barnes, S.J., Taylor, R.J.M., Kinny, P.D. and Fritz, H., 2018. A relic of the
1513 Mozambique Ocean in south-east Tanzania. *Precambrian Research*, 305: 386-426.
- 1514 Möller, A., Mezger, K. and Schenk, V., 2000. U-Pb dating of metamorphic minerals: Pan-
1515 African metamorphism and prolonged slow cooling of high pressure granulites in
1516 Tanzania, East Africa. *Precambrian Research*, 104: 123-146.
- 1517 Moore, J.M., 1979. Tectonics of the Najd Transcurrent Fault System, Saudi Arabia. *Journal of*
1518 *the Geological Society*, 136(4): 441-452.

- 1519 Muhongo, S., 1994. Neoproterozoic Collision Tectonics In the Mozambique Belt Of East- Africa
1520 - Evidence From the Uluguru Mountains, Tanzania. *Journal Of African Earth Sciences*,
1521 19: 153-168.
- 1522 Muhongo, S., Kröner, A. and Nemchin, A.A., 2001. Single zircon evaporation and SHRIMP
1523 ages for granulite-facies rocks in the Mozambique belt of Tanzania. *Journal of Geology*,
1524 109: 171-189.
- 1525 Nance, R.D., Worsley, T.R. and Moody, J.B., 1988. The Supercontinent Cycle. *Scientific*
1526 *American*, 259(1): 72-79.
- 1527 Nettle, D., Halverson, G.P., Cox, G.M., Collins, A.S., Schmitz, M., Gehling, J., Johnson, P.R.
1528 and Kadi, K., 2014. A middle-late Ediacaran volcano-sedimentary record from the
1529 eastern Arabian-Nubian shield. *Terra Nova*, 26(2): 120-129.
- 1530 Neves, S.P., Bruguier, O., Vauchez, A., Bosch, D., da Silva, J.M.R. and Mariano, G., 2006.
1531 Timing of crust formation, deposition of supracrustal sequences, and Transamazonian
1532 and Brasiliano metamorphism in the East Pernambuco belt (Borborema Province, NE
1533 Brazil): Implications for western Gondwana assembly. *Precambrian Research*, 149(3-4):
1534 197-216.
- 1535 Nutman, A.P., Mohajjel, M., Bennett, V.C. and Fergusson, C.L., 2014. Gondwanan Eoarchean-
1536 Neoproterozoic ancient crustal material in Iran and Turkey: zircon U-Pb-Hf isotopic
1537 evidence. *Canadian Journal of Earth Sciences*, 51(3): 272-285.
- 1538 Pandit, M.K., Carter, L.M., Ashwal, L.D., Tucker, R.D., Torsvik, T.H., Jamtveit, B. and
1539 Bhushan, S.K., 2003. Age, petrogenesis and significance of 1 Ga granitoids and related
1540 rocks from the Sendra area, Aravalli Craton, NW India. *Journal of Asian Earth Sciences*,
1541 22: 363-381.
- 1542 Park, Y., Swanson-Hysell, N.L., MacLennan, S.A., Maloof, A.C., Gebreslassie, M., Tremblay,
1543 M.M., Schoene, B., Alene, M., Anttila, E.S.C., Tesema, T. and Haileab, B., 2019. The
1544 lead-up to the Sturtian Snowball Earth: Neoproterozoic chemostratigraphy time-
1545 calibrated by the Tambien Group of Ethiopia. *GSA Bulletin*, 132(5-6): 1119-1149.
- 1546 Plavsa, D., Collins, A.S., Foden, J.D. and Clark, C., 2015. The evolution of a Gondwanan
1547 collisional orogen: A structural and geochronological appraisal from the Southern
1548 Granulite Terrane, South India. *Tectonics*, 34(5): 820-857.
- 1549 Plavsa, D., Collins, A.S., Foden, J.F., Kropinski, L., Santosh, M., Chetty, T.R.K. and Clark, C.,
1550 2012. Delineating crustal domains in Peninsular India: Age and chemistry of
1551 orthopyroxene-bearing felsic gneisses in the Madurai Block. *Precambrian Research*, 198:
1552 77-93.
- 1553 Plavsa, D., Collins, A.S., Payne, J.L., Foden, J.D., Clark, C. and Santosh, M., 2014. Detrital
1554 Zircons in Basement Metasedimentary Protoliths Unveil the Origins of Southern India.
1555 *Geological Society of America, Bulletin*, in press.
- 1556 Plunder, A., Blein, O., Isseini, M., Al-Gadam, I.O., Chevillard, M., Djedouboum, E., Lach, P.,
1557 Lahfid, A., Melleton, J., Rouzeau, O. and Vic, G., 2026. A window on the amalgamation
1558 of Western Gondwana: Geological history of the Ouaddaï massif (E. Chad). *Precambrian*
1559 *Research*, 434: 108000.
- 1560 Rajendra Prasad, B., Kesava Rao, G., Mall, D.M., Koteswara Rao, P., Raju, S., Reddy, M.S.,
1561 Rao, G.S.P., Sridher, V. and Prasad, A.S.S.S.R.S., 2007. Tectonic implications of seismic
1562 reflectivity pattern observed over the Precambrian Southern Granulite Terrain, India.
1563 *Precambrian Research*, 53: 1-10.

1564 Ramakrishnan, M., 1993. Tectonic Evolution of the Granulite Terrains of Southern India.
1565 Continental Crust of South India(25): 35-44.

1566 Ramezani, J. and Tucker, R.D., 2003. The Saghand region, central Iran: U-Pb geochronology,
1567 petrogenesis and implications for Gondwana tectonics. American Journal Of Science,
1568 303: 622-665.

1569 Rantakokko, N.E., Whitehouse, M.J., Pease, V. and Windley, B.F., 2014. Neoproterozoic
1570 evolution of the eastern Arabian basement based on a refined geochronology of the
1571 Marbat region, Sultanate of Oman. Tectonic Evolution of the Oman Mountains, 392:
1572 107-127.

1573 Raza, M., Ahmad, A.H.M., Khan, M.S. and Khan, F., 2012. Geochemistry and detrital modes of
1574 Proterozoic sedimentary rocks, Bayana Basin, north Delhi fold belt: implications for
1575 provenance and source-area weathering. International Geology Review, 54(1): 111-129.

1576 Reddy, S., Collins, A. and Mruma, A., 2003. Complex high-strain deformation in the Usagaran
1577 Orogen, Tanzania: structural setting of Palaeoproterozoic eclogites. Tectonophysics,
1578 375(1-4): 101-123.

1579 Reeves, C.V., de Wit, M.J. and Sahu, B.K., 2004. Tight reassembly of Gondwana exposes
1580 Phanerozoic shears in Africa as global tectonic players. Gondwana Research, 7: 7-20.

1581 Ries, A.C., Vearncombe, J.R., Price, R.C. and Shackleton, R.M., 1992. Geochronology and
1582 Geochemistry of the Rocks Associated with a Late Proterozoic Ophiolite in West Pokot,
1583 Nw Kenya. Journal of African Earth Sciences, 14(1): 25-36.

1584 Robinson, F.A., Foden, J.D. and Collins, A.S., 2015a. Geochemical and isotopic constraints on
1585 island arc, synorogenic, post-orogenic and anorogenic granitoids in the Arabian Shield,
1586 Saudi Arabia. Lithos, 220: 97-115.

1587 Robinson, F.A., Foden, J.D. and Collins, A.S., 2015b. Zircon Geochemical and
1588 Geochronological Constraints on Contaminated and Enriched Mantle Sources beneath the
1589 Arabian Shield, Saudi Arabia. Journal of Geology, 123(5): 463-489.

1590 Robinson, F.A., Foden, J.D., Collins, A.S. and Payne, J.L., 2014. Arabian Shield magmatic
1591 cycles and their relationship with Gondwana assembly: Insights from zircon U-Pb and Hf
1592 isotopes. Earth and Planetary Science Letters, 408: 207-225.

1593 Rosenbaum, G., 2018. The Tasmanides: Phanerozoic Tectonic Evolution of Eastern Australia.
1594 Annual Review of Earth and Planetary Sciences, Vol 46, 46: 291-325.

1595 Rossetti, F., Nozaem, R., Lucci, F., Vignaroli, G., Gerdes, A., Nasrabadi, M. and Theye, T.,
1596 2015. Tectonic setting and geochronology of the Cadomian (Ediacaran-Cambrian)
1597 magmatism in Central Iran, Kuh-e-Sarhangi region (NW Lut Block). Journal of Asian
1598 Earth Sciences, 102: 24-44.

1599 Sacchi, R., Cadoppi, P. and Costa, M., 2000. Pan-African reactivation of the Lurio segment of
1600 the Kibaran Belt system: a reappraisal from recent age determinations in northern
1601 Mozambique. Journal of African Earth Sciences, 30(3): 629-639.

1602 Santosh, M., Maruyama, S. and Sato, K., 2009. Anatomy of a Cambrian suture in Gondwana:
1603 Pacific type orogeny in southern India? Gondwana Research, 16: 321-341.

1604 Santosh, M., Tagawa, M., Taguchi, S. and Yoshikura, S., 2003. The Nagercoil Granulite Block,
1605 southern India: petrology, fluid inclusions and exhumation history. Journal of Asian
1606 Earth Sciences, 22: 131-155.

1607 Santosh, M., Tagawa, M., Yokoyama, K. and Collins, A.S., 2006. U-Pb electron probe
1608 geochronology of the Nagercoil granulites, southern India: Implications for Gondwana
1609 amalgamation. Journal of Asian Earth Sciences, 28(1): 63-80.

1610 Sassi, F.P. and Visonà, D., 1993. Relics of Granulitic Mineral Assemblages in the Northern
1611 Somali Basement. In: E. Abbate, M. Sagri and F.P. Sassi (Editors), *Geology and Mineral*
1612 *Resources of Somalia and Surrounding Regions*. Istituto Agronomico per l'Oltremare,
1613 Firenze, pp. 83-90.

1614 Sassi, F.P., Visonà, D., Ferrara, G., Gatto, G.O., Ibrahim, H.A., Said, A.A. and Tonarini, S.,
1615 1993. The Crystalline Basement of Northern Somalia: Lithostratigraphy and the
1616 Sequence of Events. In: E. Abbate, M. Sagri and F.P. Sassi (Editors), *Geology and*
1617 *Mineral Resources of Somalia and Surrounding Regions*. Istituto Agronomico per
1618 l'Oltremare, Firenze, pp. 3-40.

1619 Schandelmeier, H., Rahman, E.A., Wipfler, E., Küster, D., Utke, A. and Matheis, G., 1994. Late
1620 Proterozoic magmatism in the Nakasib suture, Red Sea Hills, Sudan. *Journal of the*
1621 *Geological Society*, 151(3): 485-497.

1622 Schmitt, R.d.S., Fragoso, R.d.A. and Collins, A.S., 2018. Suturing Gondwana in the Cambrian:
1623 The Orogenic Events of the Final Amalgamation. In: S. Siegesmund, M.A.S. Basei, P.
1624 Oyhantçabal and S. Oriolo (Editors), *Geology of Southwest Gondwana*. Springer
1625 International Publishing, Cham, pp. 411-432.

1626 Schoff, W.H., 1912. *The Periplus of the Erythraean sea; travel and trade in the Indian Ocean*.
1627 Longmans, Green, and Co., New York, 323 p. pp.

1628 Schreurs, G., Giese, J., Berger, A. and Gnos, E., 2010. A new perspective on the significance of
1629 the Ranotsara shear zone in Madagascar. *International Journal of Earth Sciences*, 99(8):
1630 1827-1847.

1631 Scotese, C.R., 2021. An Atlas of Phanerozoic Paleogeographic Maps: The Seas Come In and the
1632 Seas Go Out. *Annual Review Earth and Planetary Sciences*, 49: 679-728.

1633 Şengör, A.M.C., Lom, N., Zabcı, C., Sunal, G. and Öner, T., 2020. Reconstructing orogens
1634 without biostratigraphy: The Saharides and continental growth during the final assembly
1635 of Gondwana-Land. *Proceedings of the National Academy of Sciences*, 117(51): 32278-
1636 32284.

1637 Shackleton, R.M., 1996. The final collision between East and West Gondwana; where is it?
1638 *Journal of African Earth Sciences*, 23: 271-287.

1639 Shakoor, M.A., Yang, X.Y., Deng, J.H. and Hakro, A.A.A.D., 2019. Early Neoproterozoic
1640 evolution of Southeast Pakistan: evidence from geochemistry, geochronology, and
1641 isotopic composition of the Nagarparkar Igneous Complex. *International Geology*
1642 *Review*, 61(11): 1391-1408.

1643 Shellnutt, J.G., Pham, N.H.T., Denyszyn, S.W., Yeh, M.-W. and Lee, T.-Y., 2017. Timing of
1644 collisional and post-collisional Pan-African Orogeny silicic magmatism in south-central
1645 Chad. *Precambrian Research*, 301: 113-123.

1646 Shellnutt, J.G., Yeh, M.-W. and Lee, T.-Y., 2026. Is the continental crust of North-Central Africa
1647 a metacraton or a shield terrane?: the view from Chad. *Journal of African Earth Sciences*,
1648 233: 105875.

1649 Shen, C., Schmitz, M., Johnson, P., Davies, J.H.F.L. and Halverson, G.P., 2022. U-Pb
1650 geochronology and cyclostratigraphy of the middle Ediacaran upper Jibalah Group,
1651 eastern Arabian Shield. *Precambrian Research*, 375.

1652 Shields, G.A., 2007. A normalised seawater strontium isotope curve: possible implications for
1653 Neoproterozoic-Cambrian weathering rates and the further oxygenation of the Earth.
1654 *eEarth*, 2(2): 35-42.

1655 Sommer, H., Kröner, A., Hauzenberger and Muhongo, S., 2003. Metamorphic petrology and
1656 zircon geochronology of high-grade rocks from the central Mozambique belt of Tanzania.
1657 *Journal of Metamorphic Geology*, 21: 915-934.

1658 Squire, R.J., Campbell, I.H., Allen, C.M. and Wilson, C.J.L., 2006. Did the Transgondwanan
1659 Supermountain trigger the explosive radiation of animals on Earth? *Earth and Planetary*
1660 *Science Letters*, 250(1-2): 116-133.

1661 Stampfli, G.M., 2005. Plate tectonics of the Apulia-Adria Microcontinents. In: I.R. Finetti
1662 (Editor), *CROP PROJECT: Deep Seismic Exploration of the Central Mediterranean and*
1663 *Italy*. Elsevier, Amsterdam.

1664 Stern, R.J., 1994. Arc Assembly and continental collision in the Neoproterozoic East African
1665 orogeny - implications for the consolidation of Gondwana. *Annual Review of Earth and*
1666 *Planetary Sciences*, 22: 319-351.

1667 Stern, R.J. and Johnson, P., 2010. Continental lithosphere of the Arabian Plate: A geologic,
1668 petrologic, and geophysical synthesis. *Earth-Science Reviews*, 101(1-2): 29-67.

1669 Stoesser, D.B. and Frost, C.D., 2006. Nd, Pb, Sr, and O isotopic characterization of Saudi Arabian
1670 shield terranes. *Chemical Geology*, 226(3-4): 163-188.

1671 Swanson-Hysell, N.L., Maloof, A.C., Condon, D.J., Jenkin, G.R.T., Alene, M., Tremblay, M.M.,
1672 Tesema, T., Rooney, A.D. and Haileab, B., 2015. Stratigraphy and geochronology of the
1673 Tambien Group, Ethiopia: Evidence for globally synchronous carbon isotope change in
1674 the Neoproterozoic. *Geology*, 43(4): 323-326.

1675 Swanson-Hysell, N.L., Zhang, Y.M., Macdonald, F.A., Koran, I., Tasistro-Hart, A.R. and Jay,
1676 A.F., 2025. Oman was on the northern margin of a wide late Tonian Mozambique Ocean.
1677 *Geology*, 53(11).

1678 Tamblyn, R., Hand, M., Simpson, A., Gilbert, S., Wade, B. and Glorie, S., 2022. laser ablation
1679 Lu-Hf geochronology of garnet across the Western Gneiss Region: campaign-style dating
1680 of metamorphism. *Journal of the Geological Society*, 179(4).

1681 Tang, M., Chu, X., Hao, J. and Shen, B., 2021. Orogenic quiescence in Earth's middle age.
1682 *Science*, 371(6530): 728-731.

1683 Taylor, R.J.M., Clark, C., Fitzsimons, I.C.W., Santosh, M., Hand, M., Evans, N. and McDonald,
1684 B., 2014. Post-peak, fluid-mediated modification of granulite facies zircon and monazite
1685 in the Trivandrum Block, southern India. *Contributions to Mineralogy and Petrology*,
1686 168(2).

1687 Teklay, M., Kröner, A., Mezger, K. and Oberhänsli, R., 1998. Geochemistry, Pb-Pb single zircon
1688 ages and Nd-Sr isotope composition of Precambrian rocks from southern and eastern
1689 Ethiopia: implications for crustal evolution in East Africa. *Journal of African Earth*
1690 *Sciences*, 26: 207-227.

1691 Tenczer, V., Hauzenberger, C., Fritz, H., Hoinkes, G., Muhongo, S. and Klotzli, U., 2013.
1692 Crustal age domains and metamorphic reworking of the deep crust in Northern-Central
1693 Tanzania: a U/Pb zircon and monazite age study. *Mineralogy and Petrology*, 107(5): 679-
1694 707.

1695 Thomas, R.J., De Waele, B., Schofield, D.I., Goodenough, K.M., Horstwood, M., Tucker, R.D.,
1696 Bauer, W., Annells, R., Howard, K., Walsh, G., Rabarimanana, M., Rafahatelo, J.-M.,
1697 Ralison, A.V. and Randriamananjara, T., 2009. Geological evolution of the
1698 Neoproterozoic Bemarivo Belt, northern Madagascar. *Precambrian Research*, 172: 279-
1699 300.

1700 Thomas, R.J., Ellison, R.A., Goodenough, K.M., Roberts, N.M.W. and Allen, P.A., 2015. Salt
1701 domes of the UAE and Oman: Probing eastern Arabia. *Precambrian Research*, 256: 1-16.
1702 Torsvik, T.H., Ashwal, L.D., Tucker, R.D. and Eide, E.A.P.R., 2001. Geochronology and
1703 paleomagnetism of the Seychelles microcontinent: The India link. *Precambrian Research*,
1704 110: 47-59.
1705 Torsvik, T.H. and Cocks, L.R.M., 2013. New global palaeogeographical reconstructions for the
1706 Early Palaeozoic and their generation. *Early Palaeozoic Biogeography and*
1707 *Palaeogeography*, 38: 5-24.
1708 Toteu, S.F., de Wit, M., Penaye, J., Drost, K., Tait, J.A., Bouyo, M.H., Van Schmus, W.R.,
1709 Jelsma, H., Moloto-A-Kenguemba, G.R., da Silva, A.F., Lerouge, C. and Doucouré, M.,
1710 2022. Geochronology and correlations in the Central African Fold Belt along the northern
1711 edge of the Congo Craton: New insights from U-Pb dating of zircons from Cameroon,
1712 Central African Republic, and south-western Chad. *Gondwana Research*, 107: 296-324.
1713 Tucker, R.D., Amelin, Y., Belcher, R.W., Delor, C., Goncalves, P., Rabarimanana, M.H. and
1714 Ralison, A.V., 2011. Neoproterozoic extension in the Greater Dharwar Craton: a
1715 reevaluation of the "Betsimisaraka suture" in Madagascar. *Canadian Journal Of Earth*
1716 *Sciences*, 48: 389-417.
1717 Tucker, R.D., Ashwal, L.D., Handke, M.J., Hamilton, M.A., Le Grange, M. and Rambelison,
1718 R.A., 1999. U–Pb geochronology and isotope geochemistry of the Archean and
1719 Proterozoic rocks of north-central Madagascar. *Journal of Geology*, 107: 135-153.
1720 Tucker, R.D., Ashwal, L.D. and Torsvik, T.H., 2001. U-Pb geochronology of Seychelles
1721 granitoids: a Neoproterozoic continental arc fragment. *Earth and Planetary Science*
1722 *Letters*, 187: 27-38.
1723 Tucker, R.D., Roig, J.Y., Moine, B., Delor, C. and Peters, S.G., 2014. A geological synthesis of
1724 the Precambrian shield in Madagascar. *Journal of African Earth Sciences*, 94: 9-30.
1725 Ustaomer, P.A., Ustaomer, T., Collins, A.S. and Robertson, A.H.F., 2009. Cadomian (Ediacaran-
1726 Cambrian) arc magmatism in the Bitlis Massif, SE Turkey: Magmatism along the
1727 developing northern margin of Gondwana. *Tectonophysics*, 473(1-2): 99-112.
1728 Vail, J.R., 1985. Pan-African (late Precambrian) tectonic terrains and the reconstruction of the
1729 Arabian-Nubian Shield. *Geology*, 13: 839-842.
1730 Van Lente, B., Ashwal, L.D., Pandit, M.K., Bowring, S.A. and Torsvik, T.H., 2009.
1731 Neoproterozoic hydrothermally altered basaltic rocks from Rajasthan, northwest India:
1732 Implications for late Precambrian tectonic evolution of the Aravalli Craton. *Precambrian*
1733 *Research*, 170(3-4): 202-222.
1734 Vearncombe, J.R., 1983. A Proposed Continental-Margin in the Precambrian of Western Kenya.
1735 *Geologische Rundschau*, 72(2): 663-670.
1736 Veizer, J., Ala, D., Azmy, K., Bruckschen, P., Buhl, D., Bruhn, F., Carden, G.A.F., Diener, A.,
1737 Ebneth, S., Godderis, Y., Jasper, T., Korte, C., Pawellek, F., Podlaha, O.G. and Strauss,
1738 H., 1999. $^{87}\text{Sr}/^{86}\text{Sr}$, $\delta^{13}\text{C}$ and $\delta^{18}\text{O}$ evolution of Phanerozoic seawater. *Chemical*
1739 *Geology*, 161(1): 59-88.
1740 Vincent, V.I., Torremans, K., Subarkah, D., Gilbert, S.E., Farkaš, J., Collins, A.S., Stacey, J.,
1741 Doran, A.L., Jones, S. and Hitzman, M.W., 2026. In situ Rb–Sr geochronology records
1742 multiple fluid pulses in Neoproterozoic sequences from the Lubambe-Mingomba Cu
1743 deposits in the Zambian Copperbelt. *Precambrian Research*, 437: 108059.
1744 Viola, G., Henderson, I.H.C., Bingen, B., Thomas, R.J., Smethurst, M.A. and de Azavedo, S.,
1745 2008. Growth and collapse of a deeply eroded orogen: Insights from structural,

1746 geophysical, and geochronological constraints on the Pan-African evolution of NE
1747 Mozambique. *Tectonics*, 27(5).

1748 Vollstaedt, H., Eisenhauer, A., Wallmann, K., Bohm, F., Fietzke, J., Liebetrau, V., Krabbenhoft,
1749 A., Farkas, J., Tomasovych, A., Raddatz, J. and Veizer, J., 2014. The Phanerozoic delta
1750 Sr-88/86 record of seawater: New constraints on past changes in oceanic carbonate
1751 fluxes. *Geochimica Et Cosmochimica Acta*, 128: 249-265.

1752 von Raumer, J.F., Stampfli, G.A. and Bussy, F., 2003. Gondwana-derived microcontinents - the
1753 constituents of the Variscan and Alpine collisional orogens. *Tectonophysics*, 365(1-4): 7-
1754 22.

1755 Wang, W., Cawood, P.A., Zhou, M.F., Pandit, M.K., Xia, X.P. and Zhao, J.H., 2017. Low-delta
1756 O-18 Rhyolites From the Malani Igneous Suite: A Positive Test for South China and NW
1757 India Linkage in Rodinia. *Geophysical Research Letters*, 44(20): 10298-10305.

1758 Wegener, A., 1912. Die Entstehung der Kontinente. *Geologische Rundschau*, 3(4): 276-292.

1759 Westerhof, A.B.P., Härmä, P., Isabirye, E., Katto, E., Koistinen, T., Kuosmanen, E., Lehto, T.,
1760 Lehtonen, M.I., Mäkitie, H., Manninen, T., Mänttari, I., Pekkala, Y., Pokki, J., Saalman,
1761 K. and Virransalo, P., 2014. Geology and Geodynamic Development of Uganda with
1762 Explanation of the 1:1,000,000 Scale Geological Map. Geological Survey of Finland,
1763 Special Paper, Geological Survey of Finland.

1764 Whitehouse, M.J., Flowerdew, M.J., Petersson, A., Al-Khribash, S. and Stoeser, D.B., 2025. The
1765 Amlah terrane, Yemen – a missing link in the Neoproterozoic tectonic collage of the
1766 Arabian Shield. *Geological Society, London, Special Publications*, 550(1): SP550-2024-
1767 128.

1768 Whitehouse, M.J., Flowerdew, M.J., Stoeser, D.B. and Stacey, J.S., 2023. The Khida terrane -
1769 Isotopic evidence for Paleoproterozoic to Neoproterozoic basement in the eastern Arabian
1770 Shield. *Precambrian Research*, 399.

1771 Whitehouse, M.J., Pease, V. and Al-Khribash, S., 2016. Neoproterozoic crustal growth at the
1772 margin of the East Gondwana continent - age and isotopic constraints from the
1773 easternmost inliers of Oman. *International Geology Review*, 58(16): 2046-2064.

1774 Whitehouse, M.J., Windley, B.F., Ba-Bttat, M.A.O., Fanning, C.M. and Rex, D.C., 1998. Crustal
1775 evolution and terrane correlation in the eastern Arabian Shield, Yemen: geochronological
1776 constraints. *Journal of the Geological Society*, 155: 281-295.

1777 Whitehouse, M.J., Windley, B.F., Stoeser, D.B., Al-Khribash, S., Ba-Bttat, M.A.O. and Haider,
1778 A., 2001. Precambrian basement character of Yemen and correlations with Saudi Arabia
1779 and Somalia. *Precambrian Research*, 105(2-4): 357-369.

1780 Windley, B.F., Whitehouse, M.J. and BaBttat, M.A.O., 1996. Early precambrian gneiss terranes
1781 and Pan-African island arcs in Yemen: Crustal accretion of the eastern Arabian Shield.
1782 *Geology*, 24(2): 131-134.

1783 Xiao, W.J., Song, D.F., Windley, B.F., Li, J.L., Han, C.M., Wan, B., Zhang, J., Ao, S.J. and
1784 Zhang, Z.Y., 2020. Accretionary processes and metallogenesis of the Central Asian
1785 Orogenic Belt: Advances and perspectives. *Science China-Earth Sciences*, 63(3): 329-
1786 361.

1787 Yang, B., Collins, A.S., Cox, G.M., Jarrett, A.J.M., Denyszyn, S., Blades, M.L., Farkaš, J. and
1788 Glorie, S., 2020. Using Mesoproterozoic Sedimentary Geochemistry to Reconstruct
1789 Basin Tectonic Geography and Link Organic Carbon Productivity to Nutrient Flux from a
1790 Northern Australian Large Igneous Province. *Basin Research*, 32.

- 1791 Yeshanew, F.G., Pease, V., Abdelsalam, M.G. and Whitehouse, M.J., 2017. Zircon U-Pb ages,
1792 delta O-18 and whole-rock Nd isotopic compositions of the Dire Dawa Precambrian
1793 basement, eastern Ethiopia: implications for the assembly of Gondwana. *Journal of the*
1794 *Geological Society*, 174(1): 142-156.
- 1795 Yeshanew, F.G., Pease, V., Whitehouse, M.J. and Al-Khirbash, S., 2015. Zircon U-Pb
1796 geochronology and Nd isotope systematics of the Abas terrane, Yemen: Implications for
1797 Neoproterozoic crust reworking events. *Precambrian Research*, 267: 106-120.
- 1798 Zhang, W., Pease, V., Whitehouse, M.J., El-Sankary, M.M. and Shalaby, M.H., 2019. Pre-
1799 Neoproterozoic basement evolution of southwestern Egypt. *International Geology*
1800 *Review*, 61(15): 1909-1926.
- 1801 Zhou, J., Farahbakhsh, E., Williams, S., Li, X., Liu, Y., Li, S. and Müller, R.D., 2025. Machine
1802 Learning and Big Data Mining Reveal Earth's Deep Time Crustal Thickness and Tectonic
1803 Evolution: A New Chemical Mohometry Approach. *Journal of Geophysical Research:*
1804 *Solid Earth*, 130(5): e2024JB030404.
- 1805 Zhu, Z., Campbell, I.H., Allen, C.M., Brocks, J.J. and Chen, B., 2022. The temporal distribution
1806 of Earth's supermountains and their potential link to the rise of atmospheric oxygen and
1807 biological evolution. *Earth and Planetary Science Letters*, 580: 117391.
- 1808 Zoleikhaei, Y., Cawood, P.A. and Mulder, J.A., 2025. Non-arc setting for "Cadomian"
1809 magmatism in Iran and Anatolia. *Geoscience Frontiers*, 16(2): 101995.
- 1810 Zuza, A. V., Levy, D. A., and Mulligan, S. R., 2022, Geologic field evidence for non-lithostatic
1811 overpressure recorded in the North American Cordillera hinterland, northeast Nevada,
1812 *Geosci. Frontiers*, 13, 101099, doi: 10.1016/j.gsf.2020.10.006.